12-2022

Encapsulation of Antimicrobial Peptides in Bicontinuous Microemulsions for Topical Delivery to Surgical Site Infections and Chronic Wounds

Madison A. Oehler
moehler@vols.utk.edu

To the Graduate Council:

I am submitting herewith a thesis written by Madison A. Oehler entitled "Encapsulation of Antimicrobial Peptides in Bicontinuous Microemulsions for Topical Delivery to Surgical Site Infections and Chronic Wounds." I have examined the final electronic copy of this thesis for form and content and recommend that it be accepted in partial fulfillment of the requirements for the degree of Master of Science, with a major in Biosystems Engineering.

<div align="right">Douglas G. Hayes, Major Professor</div>

We have read this thesis and recommend its acceptance:

Doris D'Souza, Xiaofei Ye

<div align="right">Accepted for the Council:</div>
<div align="right"><u>Dixie L. Thompson</u></div>

<div align="right">Vice Provost and Dean of the Graduate School</div>

(Original signatures are on file with official student records.)

Encapsulation of Antimicrobial Peptides in Bicontinuous Microemulsions for Topical Delivery to Surgical Site Infections and Chronic Wounds

A Thesis Presented for the
Master of Science
Degree
The University of Tennessee, Knoxville

Madison Oehler
December 2022

Dedication

I would like to dedicate this thesis to my grandmother who recently passed away but supported my research and was excited to see the outcomes of this project.

Acknowledgements

I am extremely grateful for my mom, dad, sisters, and grandparents for their unconditional love and support over the past two years. This endeavor would never have been possible without the guidance of this project from my advisor Dr. Hayes. I would like to thank Dr. D'Souza for guiding me through the microbiology lab and being patient with me as I learned new laboratory techniques. I am also appreciative for the help of my committee member Dr. Ye. I'd like to acknowledge Oak Ridge National Laboratory for the use of their equipment and help from Wim Bras, Manju Mudiyanselage, and Viswanathan Gurumoorthy. Many thanks to the National Institute of Health for the grant towards funding this research.

Abstract

Surgical site infections and chronic wounds, especially those caused by antibiotic-resistant microorganisms, result in hospitalization and fatalities each year. Methods to prevent these infections, such as cleaning and preparing medical tools, have had minimal success in preventing infections. Further, antibiotic treatments have become less successful in treating infections and wounds because of antibiotic-resistant bacteria. Antimicrobial peptides (AMP) are a possible treatment solution for wound infections. AMPs are oligopeptides that occur in nature or can be synthesized *in vitro* which possess a broad spectrum of antimicrobial activity against bacteria and other harmful microorganisms. AMPs operate by disrupting the packing arrangements of biomembranes in prokaryotes through their insertion into negatively charged phospholipid bilayers. However, many AMP products fail clinical trials because of their difficulty to be encapsulated and delivered at high concentrations in an active form. This project proposed the use of bicontinuous microemulsions (BMEs) as a possible system to encapsulate and deliver AMPs. BMEs are thermodynamically stable mixtures consisting of a surfactant, oil, aqueous mixture, and sometimes a cosurfactant. They are optically clear and the surfactant(s) in BMEs solubilize nearly equal amounts of oil and water creating elongated nanodomains. AMPs are typically cationic, and the following hypothesis was tested: BMEs created with anionic surfactants would induce a more highly folded, hence more biologically active, conformation for melittin. Several different BME systems composed of biocompatible oils were identified and evaluated for their ability to encapsulate melittin, a model AMP, and to test the system's antimicrobial activity. Small-angle x-ray scattering showed melittin effected the BMEs quasi-periodic repeat distance and correlation lengths. Circular dichroism data showed a higher percentage of melittin was in its active form when encapsulated in a BME compared to an aqueous solution. Fluorescence measurements showed melittin resided within the surfactant monolayers of the BMEs. Antimicrobial diffusion assays proved that there was a larger zone of inhibition against bacteria commonly found in surgical site infections and chronic wounds than the BMEs without melittin. This research was successful in adding an AMP into BMEs created with biocompatible materials and may be a viable option in combating the rise in antibiotic-resistant organisms.

Table of Contents

List of Tables

List of Figures

CHAPTER 1: INTRODUCTION

1.1 Problem Overview

Within the United States (US), surgical site infections (SSIs) and chronic wounds contribute to increased treatment costs and hospital stays each year. Costs for SSIs and chronic wounds are 9 and 50 billion U.S. dollars respectively. High costs and patient discomfort provide the motivation to develop new therapeutic methods (Zimlickman et al., 2013; Fife et al., 2012). SSIs are defined as any infection that arises "within 30 days after a surgical procedure and typically occurs at the site of incision," (Gupta et al., 2021). SSIs are caused by Gram-negative and Gram-positive bacteria that originate from the patient or the external environment (Gupta et al., 2021). Health care providers and patients they treat are both at risk of contracting an SSI during any treatment or care given to the patient. Although patients are at a higher risk during or after a surgical procedure, SSIs can also be contracted from ventilators, human contact, or infected hospital rooms (Leaper, 2010). Both Bagnall et al., (2009) and Leaper (2010) claim SSIs are one of the most common healthcare associated infections but also most are preventable. Therefore, new measures are required to reduce the negative impacts resulting from SSIs. Chronic wounds are defined as wounds that do not heal in an appropriate amount of time, lasting 12-13 months or more in some cases (Frykberg and Banks, 2015). Chronic wounds may also lead to the loss of function and mobility in the area the wound resides in, resulting in an overall decrease in the quality of one's life (Frykberg and Banks, 2015). Negative impacts of both SSIs and chronic wounds include death, hospital readmission, and the emergence of antibiotic-resistant infectious microorganisms (Table 1).

There are a few ways to prevent SSIs from occurring. Before an operation, guides to reduce the risk of SSIs should be given to patients. Patients can reduce their risk of SSIs by stopping smoking, improving their diets, and ensuring their glycemic control is correct if they are diabetic (Bagnall et al., 2009). Additional guidelines were created by the National Institute for Health and Care Excellence (NICE) for prevention of surgical-site infections. Pre-operative guidelines recommend patients shower and wear appropriate clothing for operation. A nasal check should be completed to determine the non-existence of methicillin-resistant *Staphylococcus aureus* (MRSA) (Bagnall et al., 2009). When appropriate, antibiotics may be given before treatment has begun. During operations NICE guidelines require health care

2

Table 1. Significant Statistics: SSIs, chronic wounds, and anti-biotic resistant microorganisms

SSIs
• Account for 33.7% of health care-associated infections
• Deaths occur in 3% of patients with SSIs

Chronic Wounds

• 6.5 million patients affected in the US each year
• 24% of hospital readmission are wound related

Antibiotic-Resistant Microorganisms

• Affect 5-10% hospitalized patients
• Methicillin-resistant *Staphylococcus aureus* (MRSA) associated with 94,300 cases/year

(AHRQ, 2019; Fife et al., 2012)

providers to use disposable materials, wear sterile gloves, and maintain patient temperature and optimal oxygen, and more (Bagnall et al., 2009). After surgery, care should be taken to change dressings and cleanse the wound up to 48 hours after completion. They state topical antimicrobials, gauze, and antiseptics should not be used while the wound is healing. If these measures do not work and an SSI is suspected, NICE suggests giving the patient an antibiotic to treat the wound area (Bagnall et al., 2009). Chronic wounds typically occur in people who have underlying conditions such as diabetes, malnutrition, and obesity (Sen, 2019). In an active wound, debridement is commonly used to cleanse a wound to remove unwanted skin that may delay the growth of new tissue (Liu et al., 2022; Frykberg and Banks, 2015). Drainage is used to remove infectious bacterial cultures from the wound to prevent inflammation (Liu et al., 2022). Debridement and drainage are two common ways to prevent wounds from becoming infected and chronic.

Treatments are available for SSIs and chronic wounds to reduce the longevity of their impacts. When a patient contracts an SSI, a specimen from the infection is tested to determine if there are any antibiotic resistant bacteria (Bagnall et al., 2015). After antibiotic treatment begins, it should be changed if a resistant culture is detected. Bagnall et al., (2015) stated, "over 15% of post-operative wounds are treated with antibiotics, possibly inappropriately." Other treatments should be required if health care providers are aware of an antibiotic-resistant strain within the patient's infection. Liu et al., (2022) discussed the importance of determining the proper treatment for wounds. If given the correct treatment, the patient would heal quickly, but if given the wrong treatment it may aggravate the wound or lead to additional antibiotic-resistant microorganisms. When wound infections are confirmed there are treatments including antimicrobial agents and dressings available. Healthcare providers are recommended to administer 6 weeks of antibiotic therapy such as quinolones, tetracyclines, and cephalosporins to wounds (Liu et al., 2022). However, negative impacts occur from a rise in bacterial resistance to antibiotics. Liu et al., (2022) stated, "70% of bacteria that is responsible for wound infections are resistant to at least one of the most frequently-used antibiotics." Their statement suggests a need for novel treatments to combat chronic wounds. Other treatments include antibiotic dressings, antimicrobial enzyme dressings, and silver-containing dressings. Both SSIs and chronic wounds

require new treatments to combat the rise in antibiotic-resistant microorganism due to the overuse and improper use of antibiotics.

Bacteria commonly found in surgical site infections and chronic wounds are listed in Table 2. This list consists of Gram-negative and Gram-positive bacteria. The term "Gram" originates from Christian Gram who developed a procedure to stain for the two major types of bacteria (Silhavy et al., 2010). The main difference between Gram-positive and Gram-negative bacteria is their structure. Gram-negative bacteria have an outer membrane, small peptidoglycan wall, and an inner membrane. Gram-positive bacteria do not have an outer membrane, but they have a larger peptidoglycan cell wall and a plasma membrane. Silhavy et al., (2010) describe Gram-negative bacteria as more likely to be resistant to antibiotics when compared to Gram-positive bacteria. Although Gram-negative bacteria are more likely to resist antibiotics, Gram-positive bacterium, *Streptococcus aureus,* has been known to show resistance to beta-lactam antibiotics such as methicillin. These bacteria can be aerobes, anaerobes, or facultative anaerobes. Facultative anaerobes can grow in conditions with and without oxygen.

Acinetobacter baumanii is the most common strain of *Acinetobacter* that causes infections in humans. *A. baumannii* is a Gram-negative bacterium that can be found in blood, urinary tract, lungs, and wounds. This bacterium is capable of avoiding the effects of antibiotics (CDC, 2019). *Enterococcus faecium* is a Gram-positive multi-drug resistant strain of bacterium. *Escherichia. coli* is a Gram-negative bacterium found in the environment, foods, intestines of humans, and animals. Many strains of this bacterium are of no concern to humans; however, some strains such as Shiga-toxin producing *E. coli,* can cause great illness (CDC, 2014). Some of these illnesses include diarrhea, urinary tract infection, and respiratory illness or pneumonia. *Pseudomonas aeruginosa* is a Gram-negative bacterium commonly found in soil and water. This strain of *Pseudomonas* is the most common one found to cause infections in humans. Typically, after surgery these infections can arise in the blood, lungs, or other parts of the body. Similar to the other bacteria strains mentioned, *P. aeruginosa* has found ways of avoiding antibiotic treatment of infections (CDC, 2019). *S. aureus* is a Gram-positive bacterium that is commonly found in the noses of humans. Typically, this bacterium will not cause issues, but if infected**, it** can cause infections that are fatal. *S. aureus* may cause sepsis, pneumonia, endocarditis, and osteomyelitis and some strains, such **as** MRSA, are antibiotic resistant (CDC, 2019). MRSA is

Table 2. Bacteria Commonly Found in Surgical Site Infections and Chronic Wounds

Bacteria	Properties
Acinetobacter baumannii	Aerobic, Gram-negative
Enterococcus faecium	Facultative Anaerobe, Gram-positive
Escherichia coli	Facultative Anaerobe, Gram-negative
Pseudomonas aeruginosa	Aerobic, Gram-negative
Methicillin-resistant Staphylococcus aureus (MRSA)	Facultative Anaerobic, Gram-positive
Streptococcus pyogenes	Facultative Anaerobe, Gram-positive

resistant to multiple antibiotics and the CDC, (2019) claims it to be a "serious threat." *Streptococcus pyogenes* is a human specific bacterial pathogen that can cause mild to fatal infections. This bacterium is a coccus shaped, Gram-positive facultative anaerobe that can occur in pairs or chains. This strain of *Streptococcus* is highly contagious and can occur by coming in contact to contaminated food, surfaces, skin lesions, or airborne droplets (CDC, 2021).

Literature review suggests the common theme that novel treatments are required to combat the rise in negative impacts resulting from SSIs and chronic wounds. Antimicrobial peptides (AMP) are a possible solution to treat bacteria commonly found in SSIs and chronic wounds. Research has shown problems in effectively encapsulating and delivering AMPs as a treatment. Bicontinuous microemulsions (BME) are a possible solution to encapsulate and effectively deliver an AMP to treat Gram-negative and Gram-positive bacteria. The remainder of Chapter 1 will focus on the review of AMPs, BMEs, and BME drug delivery systems. The chapter will conclude with the overlying objective for this thesis project.

1.2 Antimicrobial Peptide Background

AMPs are naturally occurring oligopeptides that originate from animals, humans, or synthetic creation. They are grouped into four main categories based on their secondary structures: alpha-helix (Fig. 1), beta-sheet, extended, and loop. There are close to 20,000 known naturally occurring and synthesized AMP's documented in the database of antimicrobial activity and structure of peptides (DBAASP) (Gogoladze et al., 2014). They are of great interest to the pharmaceutical and medical industry because of their activity and ability to function against bacteria, fungi, viruses, and tumors (Bahar and Ren, 2013). AMPs hold better mode of functions for destroying unwanted hosts, when compared to antibiotics, that are ideal for treatment of patients. Antibiotic treatments are designed to target specific cellular activities which has resulted in bacteria building a resistance to them. Bahar and Ren (2013) stated, "Unlike antibiotics, which target specific cellular activities, AMP's target the lipopolysaccharide layer of the cell membrane." AMPs function by targeting and disrupting cell membranes of the unwanted host resulting in cell death and a lesser chance of building a resistance. Therefore, AMPs have the potential to be an effective treatment for SSIs and chronic wounds.
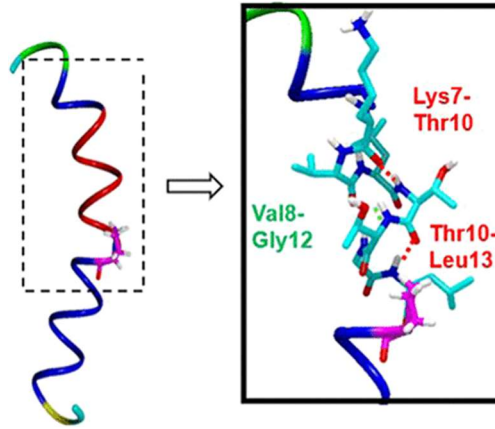
Figure 1. AMP melittin alpha-helix structure (Ramirez et al, 2019)

1.2.1 AMP Mechanism of Action

AMPs are beneficial in killing unwanted hosts because of their mechanism and way of functioning. Models were introduced to describe the mechanisms of AMPs and how they cause cell death, some are shown in Figure 2. Three common models include barrel stave, toroidal, and carpet (Teixeira et al., 2012). In the barrel-stave model, AMPs, self-assemble together on the surface of the cell and form alpha helices (Fig. 2A). When a certain threshold concentration is met, the peptides will self-aggregate and insert themselves into the membrane creating a pore. The pore size may increase with additional peptides which further induces lysis of the cell. In the carpet model, peptides bind to the anionic phospholipids by electrostatic forces resulting in coverage of the entire surface membrane (Fig. 2B). The carpet model displays of disruption of the cell surface by dispersive disruption and not channeled disruption which is seen in the toroidal pore and barrel-stave models. The toroidal pore mechanism occurs when a stable pore forms on the cell membrane causing it to leak and create cell lysis (Fig. 2C). It was described that in the molecular electroporation mechanism, a cationic peptide creates an electrical potential difference through the membrane and when a voltage of 0.2 is met, a pore forms by electroporation (Fig. 2D). The sinking raft method proposes that a curvature is created on the membrane as a result of peptide attachment and creates pores in the membrane causing permeability and leakage of the cell (Fig. 2E).

1.2.2 Model AMP's

There are thousands of known AMP's, four of which have properties listed in Table 3. Melittin and magainin-2 are two of the most studied AMPs to date. LL-37 is from human origin. And gramicidin S has a beta-sheet structure which differs from the other three AMPs.

1.2.3 Melittin

The AMP melittin is a main component of bee venom. It is an amphipathic peptide consisting of 26 amino acids, with an alpha-helix secondary structure (Fig. 1). This AMP disrupts cell membranes as well as intracellular membranes using toroidal pores by accumulating on a cell surface and disrupting the membrane to cause cell lysis (Fig. 2C). Melittin has been studied for use in many areas such as therapeutics, biotechnology, and cancer studies (Moreno
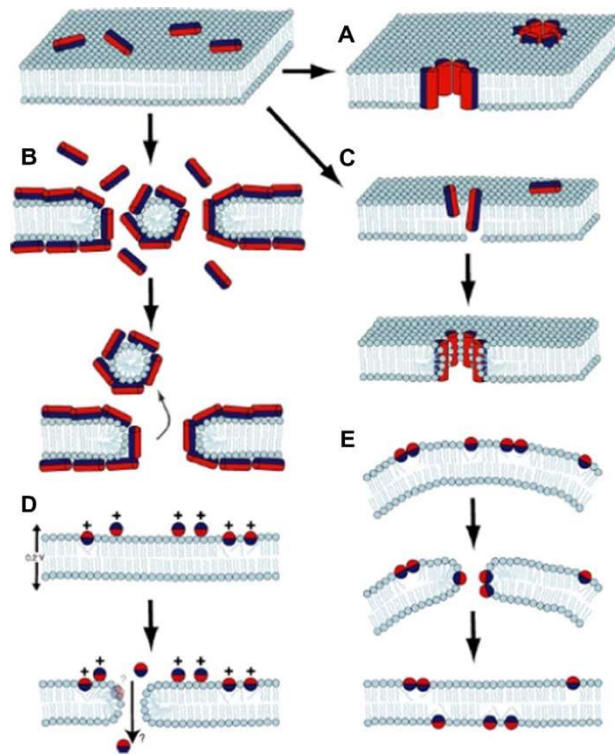
Figure 2. Mechanism of action for AMPs retrieved from Teixeira et al., 2012: a visual to describe various AMP mechanism models that have been presented. The letters in represent: (A) barrel-stave, (B) carpet, (C) toroidal, (D) molecular electroporation, and (E) sinking raft mechanism

Table 3. List of properties of the AMPs

AMP	Amino-acids	Hydrophobicity	Net charge	Secondary structure	Activity
Melittin	26	46%	+6	α-helix	Gram+/-; virus; parasites; HIV; cancer
Magainin-2	23	43%	+3	α-helix	Gram+/-; virus; parasites; HIV; cancer
LL-37	37	35%	+6	α-helix	Gram+/-; virus; fungi
Gramicidin S	10	60%	+2	β-hairpin	Gram +/-; fungi

and Giralt, 2015). Although melittin has been heavily researched, currently there are not any products with melittin for human use. One reason is that melittin, similar to other AMP's, can be cytotoxic to human red blood cells (Jamasbi et al., 2016). Though, promising research shows that the amphiphilicity of melittin makes it a suitable candidate to interact with membrane or membrane mimetic systems. Therefore, the use of microemulsions in this project should not have the issue of cytotoxicity. When melittin was in contact with a lipid micelle or membrane, its secondary structure was found to be an alpha helix, which is its most active state. This is beneficial because if melittin is successfully added to the BMEs, it will likely conform into its most active state and be effective in killing unwanted bacteria.

1.2.4 Magainin-2

Magainin-2, shown in Figure 3, is an alpha-helical AMP and antiparasitic peptide that originated from the skin of the African clawed frog, discovered in 1987 (Ramos et al., 2012). Scientists discovered magainin-2 in addition to magainin-1 after conducting experiments on frogs by creating incisions on the frog's skin and placing them into microbe filled tanks (Gottler and Ramamoorthy, 2008). The researchers discovered that something kept the frogs from getting infected, hence the discovery of magainin. Magainin-2 showed to have extensive antifungal and antibacterial activities (Gottler and Ramamoorthy, 2018) and is capable of fighting against Gram-positive and Gram-negative bacteria, fungi, and protozoa (Schäfer-Korting and Rolff, 2018). It has been shown that magainin-2 does not attack erythrocytes which is important in their development as a treatment for humans (Matsuzaki et al., 1994).

1.2.5 LL-37

LL-37, shown in Figure 4, is an alpha-helical AMP that is positively charged and originates from human skin and glands (Bucki et al., 2009). This AMP has shown "activity against Gram-negative and Gram-positive bacteria, viruses, and fungi," (van der Does et. al., 2012). Previous research has shown activities of LL-37 against *E. coli, S. aureus, methicillin-resistant S. aureus, Klebsiella pneumoniae,* and more. One of the most important activities of LL-37 is its involvement in tissue healing. LL-37 has been shown to activate endothelial cells which are linked to directly promoting skin growth. In a study using LL-37 on burned tissue, it
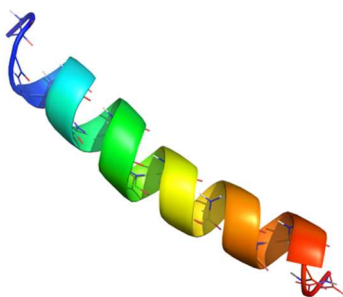
Figure 3. Structure of magainin-2 retrieved from DRAMP AMP database (Kang et al., 2019)
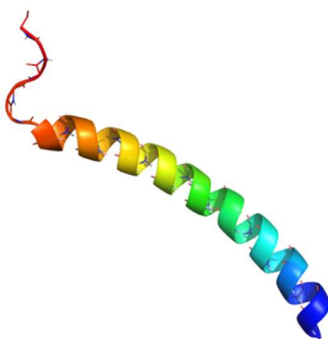
Figure 4. Structure of LL-37 retrieved from DRAMP AMP database (Kang et al., 2019)

was found that there were higher levels of mRNA in the burned tissue versus the unburned tissue (Bucki et al., 2009). This AMP would be very useful in the treatment of open wounds and tissue injuries.

1.2.6 Gramicidin S

Gramicidin is a cyclic decapeptide with a beta-sheet structure that was isolated from *Bacillus brevis*. This AMP functions against Gram-negative and Gram-positive bacteria and fungi (Mogi and Kita, 2009). Currently gramicidin has been used in topical applications as a treatment for external ear infections, throat infections, and root canal infections (Guan et al., 2019). There are many proposed models for the mode of action of gramicidin, but the most recent suggests that this AMP forms well-defined ion-channels causing the cell to lyse. Although a useful and well-known AMP, there are reports of gramicidin showing toxicity towards human red blood cells due to hydrophobic interactions. It is hopeful that the addition of gramicidin to a microemulsion would reduce the cytotoxic effects that have been reported.

1.3 Current AMP Drug Delivery Modes

Treatments containing AMPs have had minimal success in the pharmaceutical industry. AMPs have been widely studied for their mechanisms and functions, but research becomes sparse for the delivery systems of AMP's. Delivery systems for AMP's are challenging because they must take into consideration, reducing unwanted side-effects, controlling AMP release rates, promoting membrane penetration, and more (Nordstrom and Malmsten, 2017). They can be delivered to the body through the skin, orally, and other methods.

1.3.1 Pexiganan Topical Treatment for Magainin-2

One of the first AMP topical treatments tested on infected wounds, Pexiganan, used magainin-2 (Thapa et al., 2019). Pexiganan, is a topical wound treatment, consisting of an AMP based off magainin-2, that passed 3 rounds of clinical trials to aid in reducing diabetic foot ulcers, but overall did not accomplish food and drug administration (FDA) approval (Gottler and Ramamoorthy, 2008). Similarly, to previous studies, they claimed that the magainin-2 mechanism for destroying cells was by forming toroidal pores in the bacterial membranes. They

provided many results on the effectiveness of Pexiganan from their *in vitro* studies. Their results showed that 50 μg/mL was effective in reducing colony forming units/population levels of *E. coli* and *S. aureus* (Gottler and Ramamoorthy, 2008). Although this product seemed to produce beneficial results, they had difficulties in the topological aspect of preparing stable layers of Pexiganan. Eventually, this product was not viewed as being significantly better than the products readily available for foot ulcers and it did not pass the final stage of its clinical trials (Dijksteel et al., 2021).

1.3.2 Other Proposed Drug Delivery Systems for AMPs

Nordström and Malmsten (2017) reviewed the available drug delivery systems for AMP's and grouped them into six categories: inorganic materials, polymeric materials, surfactant and lipid dispersion/self-assembly systems, peptide self-assembly systems, and other formulations. Inorganic materials have the ability to protect AMPs from enzymatic degradation and control drug release. They also have antimicrobial properties which could have an additive effect when combined with an AMP. Some examples of inorganic materials include mesoporous silica, titanium, metal nanoparticles, and quantum dots. Polymeric materials have shown promising results and are compatible with a variety of AMP's (Nordstrom and Malmsten, 2017). Examples of polymeric materials include polymer particles and fibers, polymer microgels, polymer multilayers, and polymer conjugates. Surfactant systems have been tested for the transport of AMPs through micellar, reversed micelles, microemulsions, and liquid crystalline (nanoparticles). Peptide self-assembly systems, like its name incorporates peptides that self-assemble into different structures on a nano level (Nordstrom and Malmsten, 2017).

Although AMPs have many beneficial functions, such as wound healing, they have made little success in industry because of various issues including potential toxicity to humans, sensitivity to weather, folding problems, and high costs, (Thapa et al., 2019; Bahar and Ren, 2013). The difficulty in using AMPs in a clinical setting resides in the limited amount of AMP concentration that can be used before becoming a risk to people due to cytotoxicity. Additionally, AMPs cannot maintain stability on their own which limits delivery methods (Thapa et al., 2019). Therefore, new vehicles, such as bicontinuous microemulsions, require research and testing to determine an optimal topical formula that includes AMPs.

1.4 Fundamentals of Microemulsions

Microemulsions are defined as thermodynamically stable mixtures created by mixing apolar and polar liquids using surfactants, sometimes with the addition of a cosurfactant (Yuan et al., 2007). Microemulsions are often created by combining a mixture of surfactants into a chosen oil with a polar solution and mixing until fully incorporated. Occasionally, surfactants are added to the polar solution first, especially if the surfactant favors a hydrophilic environment. Because microemulsions are thermodynamically stable, their formation is not dependent on the order their components are combined. Microemulsion systems are optically clear and form many droplets when produced dependent on the type of microemulsion formed (Anil and Kannan, 2018). Microemulsions are of small size, 10-30 nm, are beneficial because they create a large surface area for drugs or peptides to reside in, which allows for a high concentration to be delivered as a treatment. Microemulsions have a variety of applications including oil recovery, protein extraction, detergents, drug delivery, and many more (Liu et al., 2009). Advantages of microemulsions include being inexpensive and easily scalable. The ability to scale is amenable for use in manufacturing (Yanyu et al., 2012; Spernath and Aserin, 2006). Other advantages of microemulsions include high drug solubilization capacity and thermodynamic stability (Tartaro et al., 2020). Additionally, they do not require large amounts of energy for production because they form spontaneously, with an added benefit of remaining stable after they are formed.

1.4.1 Emulsion Characteristics

Microemulsions are one of many surfactant-oil-water self-assembly systems that can be created. The particle sizes of microemulsions reside in the range of 10-30 nm. Although they are nanoscale, Abbott (2012) discussed how they were initially given the name microemulsion in the 1940s, prior to knowledge of nanoscale dispersions, which could not be changed. Other types of emulsions include nanoemulsions and macroemulsions. Nanoemulsions, also known as miniemulsions, differ from microemulsions as their size is between 100-400 nm and they are not thermodynamically stable. Miniemulsions are created by swelling micellar structures using a solvent to break the swollen structures into small droplets (Rosen, 1989). Macroemulsions are the standard emulsions residing in the micrometer size range and they are also thermodynamically unstable (Abbott, 2012). Vesicles are another system that are created with

surfactants, water, and small amounts of oil. Although they have similarities to microemulsions, they are not the same; vesicles consist of bilayers and microemulsions consist of monolayers (Kegel and Reiss, 1996). Figure 5 show the differences in structures between w/o and o/w microemulsions, vesicles, and bicontinuous structures. The surfactant in a w/o or o/w microemulsion forms a single layer droplet, whereas the vesicle has multiple layers within its droplet. The bicontinuous phase does not consist of spherical dispersions, but of elongated nanodomains (Fig. 5). Other structures created by surfactants are the crystalline phases which include cubic, hexagonal, and lamellar phases.

1.4.2 Surfactants

Surfactants, one of the main components of microemulsions, are defined as compounds capable of lowering the surface tension between two immiscible phases (Rosen, 1989). They are used in microemulsions to lower the surface tension between two liquid phases: oil and water. The surfactant structures consist of a hydrophilic head group and a lipophilic tail group which allow oil and water to mix. The type of surfactant used in creating a microemulsion dictates what type of system is created. Surfactants with longer lipophilic tails are strongly attracted to an oil phase and have a decreased attraction to an aqueous phase. Microemulsion systems typically consist of ionic or nonionic surfactants, and in many cases a mixture of both (Figs. 6 and 7) (Nakama, 2017). Ethoxylate (nonionic) surfactants are strongly affected by temperature, and ionic surfactants are strongly affected by the salinity of the aqueous phase (Rosen, 1989). Zwitterionic surfactants that have positive and negative charged head groups can also form microemulsions (Fig. 8). Figure 8 depicts phosphatidyl choline from lecithin, the latter of which is a mixture of other various phospholipids (Hirose et al., 2018). This project mainly focuses on the use of anionic surfactants such as Aerosol-OT (AOT), displayed in Figure 6.

1.4.3 Winsor Microemulsion Systems

There are four types of microemulsions systems discovered by Winsor in the 1950s that are referred to as Winsor systems: Winsor-I (W-I), II (W-II), III (W-III), and IV (W-IV) (Abbott, 2012; Solans and Garcia-Celma, 1997). W-IV systems are single phase systems that are composed of either an oil-in-water microemulsion, water-in-oil microemulsion, or a BME
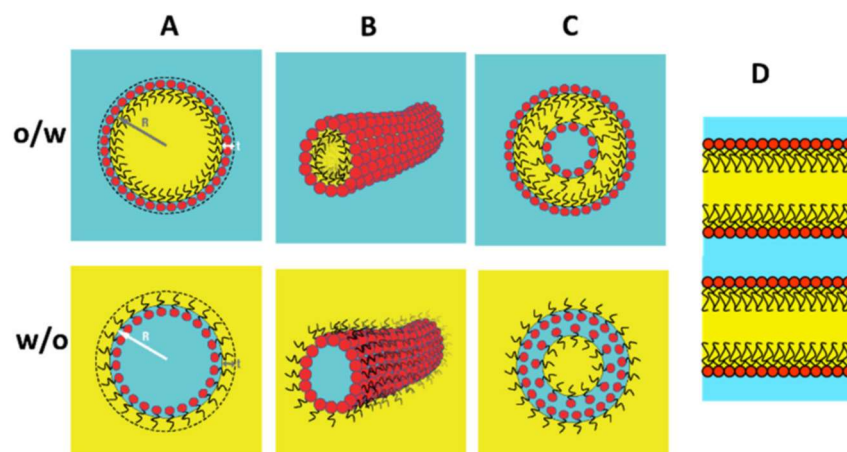
Figure 5. Surfactant-oil water self-assemble systems Diagram retrieved from Tartaro et al. (2020); yellow represents oil, blue represents water, and the red head with black tail represents the surfactant. Columns A and B display the structure of oil-in-water (o/w) and water-in-oil (w/o) microemulsions with spherical and cylindrical micelles, column C displays the structure of vesicles, and column D displays bicontinuous planar interfaces
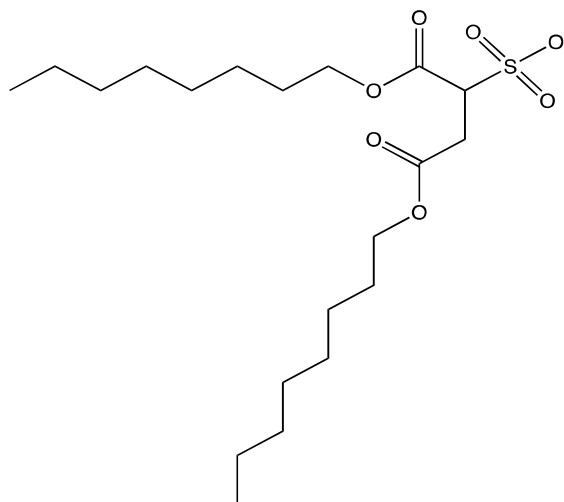
Figure 6. Structure of the anionic surfactant AOT
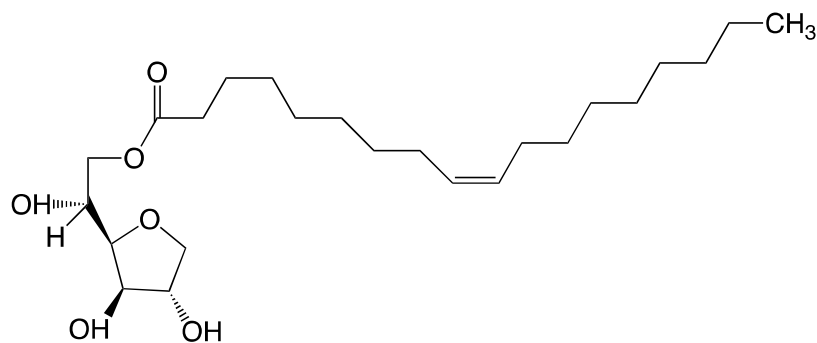
Figure 7. Structure of nonionic surfactant sorbitan monooleate
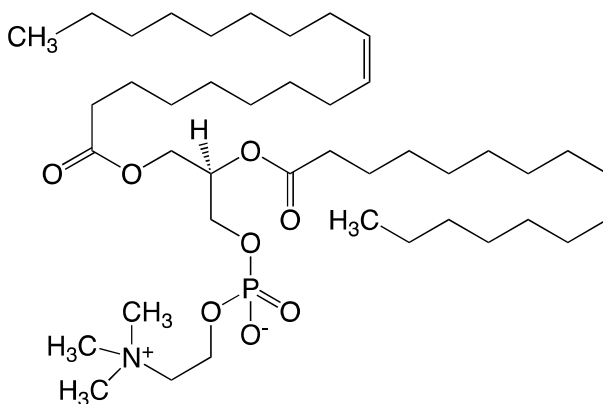
Figure 8. Structure of zwitterionic surfactant, lecithin, composed of phosphatidyl choline depicted here, and other phospholipids

(Fig. 9). When a system consists of a surfactant that favors a hydrophilic environment, the lipophilic tails drive the oil to partition into the aqueous phase, forming a one-phase system composed of oil droplets in water (o/w microemulsions). Similarly, if a surfactant favors a lipophilic environment, the hydrophilic head group drives water to partition into the oil phase, forming a one-phase system of water droplets in oil (w/o microemulsions). Unlike o/w and w/o microemulsion-based W-IV systems, a bicontinuous W-IV system occurs when the surfactant solubilizes nearly equal amounts of oil and water, forming a one phase system composed of elongated nanodomains. W-I and W-II systems are two phase systems that are similar to the oil-in-water and water-in-oil W-IV systems. A W-I system starts with surfactant dissolved in an aqueous solution. Oil is added and when the system can no longer accept more, an excess top oil phase is formed (Fig. 9). A W-II system begins with a surfactant dissolved in an oil phase. When the lipophilic surfactant no longer accepts water into the oil phase it results in an excess bottom aqueous phase (Fig. 9). The W-III system is a three phase BME. A W-III system forms when an aqueous phase is added to an oil phase with surfactants. When the surfactant(s) can no longer accept any more oil or water to the bicontinuous middle phase it results in a 3-phase system with excess oil and water phases.

1.4.4 Ternary Phase Diagram for Microemulsions

A ternary phase diagram depicts what percentage of surfactant, aqueous phase, and oil phase is required to obtain a specific Winsor system at a fixed temperature and salinity. These diagrams can be created for any system to help researchers produce specific Winsor systems for a given set of microemulsion components. In Figure 10, the red point in the depicted ternary phase diagram represents a microemulsion that would consist of 26 wt% surfactant, 38% oil, and 36% water. Studies that create ternary phase diagrams label the sections of their graph with corresponding Winsor system(s). Figure 11 shows a phase diagram from a study conducted by Tartaro et al., (2020). They labeled their diagrams with L1 and L2 which correspond with o/w and w/o microemulsions.
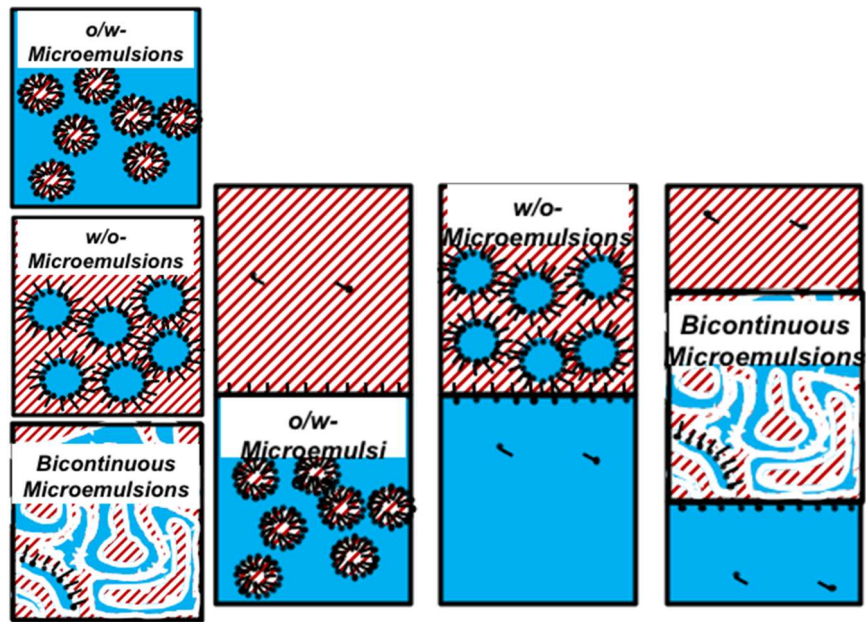
Figure 9. From left to right, diagram depicting structures of Winsor IV, I, II, and III, microemulsions; red striped represent the oil phase, blue represents the aqueous solution, and the black structures represent the surfactants (Hayes, 2013)
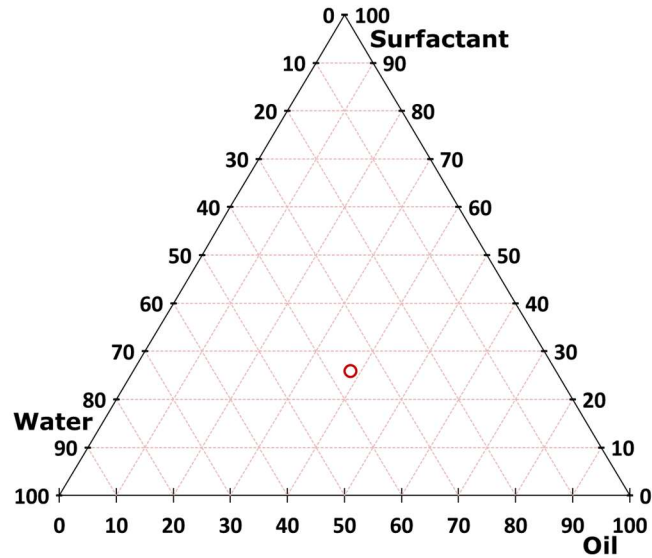
Figure 10. Example of ternary diagram shape with one data point at 26% surfactant, 38% oil, and 36% water
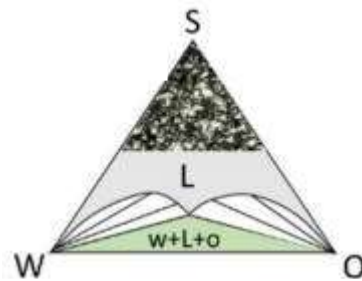
Figure 11. Diagram retrieved from Tartaro et al. (2020): ternary isothermal phase diagram at the critical temperature, L represents a liquid microemulsion, o/w and w/o are likely to occur to the left and right of the L region, and the black region at the top of the diagram represents a liquid crystalline phase

1.4.5 Fish Phase Diagram

The phase behavior of a microemulsion is dependent on the structure of the surfactant and components that affect the surfactant, mainly temperature and salinity. Kahlweit's fish diagram is used to depict the relationship of surfactant concentration to temperature or salinity of the microemulsion system (Tartaro et al., 2020). For nonionic surfactants (alkyl ethoxylate), as temperature increases, the lipophilicity of the surfactant increases (Moghaddam, 2016). For ionic surfactants, as temperature increases, the hydrophilicity of the surfactant increases. The opposite occurs for nonionic and ionic surfactants as salinity increases. For ionic surfactants, as salinity increases the surfactant becomes more hydrophilic. As salinity increases for an ionic surfactant, it becomes more lipophilic.

Figure 12 displays a fish diagram where the y-axis typically consists of temperature or salinity. Temperature and salinity are parameters used to change the properties of the surfactants to obtain different Winsor systems. The water to oil ratio is kept constant throughout the diagram and most diagrams use a ratio of 1:1 w/w. Fish diagrams are created for any system and allow researchers to determine what concentration of surfactant is required to make any Winsor system. In Figure 12, as temperature increases at a lower surfactant concentration (below Φ_s^*), the system changes from a W-I to W-III to W-II system. If the system uses a stronger concentration of an ionic surfactant, the temperature increase causes the surfactant to become more hydrophilic. Therefore, it would change from an o/w environment to a w/o environment. The change between a W-I to a W-II system is considered the "head" of the fish and is highlighted in green in Figure 12. The head represents the temperature and surfactant concentration combination that will create a W-III system for the water/oil ratio employed. The Φ_s^* value in Figure 12 represents the "neck" of the fish, or more specifically, the optimal surfactant concentration. To the right of the neck, highlighted in grey, is the tail of the fish. The tail of the fish consists of one phase W-IV systems that vary from o/w, bicontinuous, and w/o. The nature of the W-IV system changes with the tuning parameter, which in this case is temperature.
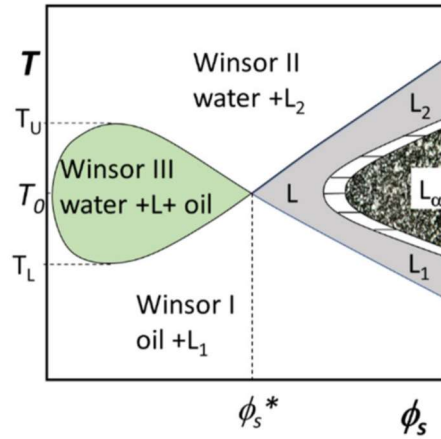
Figure 12. "Fish" diagram retrieved from Tartaro et al. (2020): with temperature on the y-axis and surfactant concentration on the x-axis. L stands for a one-phase system, L_1 is an o/w microemulsion, L_2 is a w/o microemulsion, L_∞ is the lamellar liquid crystalline phase, ϕ_s^* is the optimal surfactant concentration, T_0 is the optimal temperature, oil and water ratios are kept equal

1.4.6 Hydrophilic-lipophilic Deviation

Models have been suggested to help determine the compositions and environmental conditions that will produce a desired microemulsion type. The most accurate to date is the hydrophilic-lipophilic deviation (HLD) model (Abbott, 2012). The purpose of HLD is to predict microemulsion formulations in order to reduce the lab work required to create a microemulsion. The HLD model directly relates to thermodynamic parameters of each component of the microemulsion system. This model is represented by the equation:

$$HLD = Cc - kEACN - \alpha\Delta T + f(S) \tag{1}$$

where,

HLD= hydrophilic-lipophilic deviation
Cc= surfactant number (characteristic value)
k= EACN scaling factor, usually 0.17
EACN= effective alkane carbon number
α= 0.1 for anionic, -0.06 for ethoxylates, 0 for sugars
ΔT= change in temperature from room temperature, 25ºC
f(S)= salinity, 0.13S for nonionic, and ln(S) for ionic.

The Cc factor represents the surfactant's relative hydrophilicity and lipophilicity. When a surfactant mixture is used, mole fractions can be used to calculate the overall Cc value. The EACN number is based on the carbon number of the oil being used. The temperature factor changes based on the type of surfactant that is present. If there is a mixture of nonionic and ionic surfactants, mole fractions are used to calculate the overall α value. The α term is positive for anionic surfactants and negative for ethoxylate surfactants. Anionic surfactants are associated with a low positive α value because temperature affects anionic surfactants minimally resulting in a small decrease in HLD. A high negative α value is associated with ethoxylate surfactants because temperature has a large effect on their polyethylene oxide head groups, which rapidly increases HLD. With an increase in temperature for ethoxylate surfactants, there would be an increase in HLD. Similarly, for the salinity term, there are two functions that are used based on if the system uses a nonionic or ionic surfactant. There are two different functions because salinity affects nonionic and ionic surfactants differently. Nonionic surfactants are less affected by salinity than ionic surfactants. For a mixed surfactant system, the overall salinity term is

calculated by mole fractions of the surfactants. An HLD value less than 0 signifies a a W-I system. If the HLD is greater than 0, a W-II system should be created. Finally, with an HLD of 0 or very close to 0, a W-III system would likely be achieved.

1.5 Microemulsion as a Topical Delivery System

Currently employed drug delivery systems for proteins and peptides are often expensive and require many resources to create and test. Anil and Kannan, (2018) describe proteins and peptides delivered by: "intradermal, subcutaneous, transdermal, intravenous, and intramuscular injections." Oral delivery of peptides is commonly used; however, multiple doses are required to be effective (Anil and Kannan, 2018). Many of the available delivery methods induce protein denaturation and degradation after formation. Further, many of these methods are invasive and minimally effective. Topical delivery is a non-invasive drug delivery method that will be discussed further as a potential method to delivery AMP loaded microemulsions.

A more favorable route of delivery is topical delivery because the skin is the largest and most accessible organ of the human body (Goebel and Neubert, 2008). Although favored, topical delivery is difficult because the top layer of skin does not allow for many foreign molecules to enter. Though difficult, Goebel and Neubert (2008) described multiple systems that were successful for the delivery of proteins. One system, iontophoresis, delivers peptides using an electric field. Though successful, this approach is not practical for patients who would use this at home. Other similar techniques of non-invasive delivery include electroporation and sonophoresis. But similar to iontophoresis, these methods are not practical for at home users. Microemulsions are of high interest to scientists because of the possible use as a topical delivery vehicle.

1.5.1 Microemulsion as a Topical Drug Delivery System

Microemulsions are a potential drug delivery system that can be applied topically to the skin. Microemulsion components can be chosen to be biocompatible with the skin. They are typically inexpensive and scalable and have shown an increase in drug absorption when applied to the skin (Kumar and Pravallika, 2019). In recent years, researchers tested ways to use microemulsions to encapsulate proteins, peptides, and other drugs for delivery (Pachuau, 2015).

They learned microemulsions offer longer shelf lives in addition to using biocompatible materials. Additionally, BMEs in particular have been shown to solubilize larger quantities of drugs because of their hydrophilic and lipophilic phases (Yuan et al., 2007). Solubilization of larger quantities, resulting from the high-volume fractions of water and oil, allow for a more significant treatment of the chosen drug.

Microemulsions employed for pharmaceutical use are commonly made with nonionic or zwitterionic surfactants. Research was conducted using W-I and W-II microemulsions for topical delivery of prostaglandin E1 (Lawrence and Rees, 2000). However, their systems did not have adequate penetration rates for this drug. Another study used lecithin microemulsions to deliver indomethacin and diclofenac. But the investigators discovered through spectroscopy an inconsistency in structure in the human stratum corneum after 24 hours of incubation (Lawrence and Rees, 2000). Other studies used w/o or o/w microemulsions to deliver drugs, including but not limited to felodipine, diphenhydramine hydrochloride, and piroxicam (Lawrence and Rees, 2000).

Other researchers studied W-IV bicontinuous systems for the delivery of various drugs. A microemulsion system containing aerosol-OT (AOT), Tween 85, isopropyl myristate (IPM), and water was tested for the transdermal delivery of 5-fluorouracil (Yanyu et al., 2012). Their study used W-IV systems to incorporate their chosen drug. This system was significant because they used a mixed nonionic-anionic surfactant mixture of Tween 85 and AOT. Additionally, they used a biocompatible oil, IPM, and the microemulsions formed at room temperature. Klossek et al., (2013) conducted a study that used a microemulsion system with components that included sodium oleate, citronellol, ethanol, limonene, and water. This system differed from the other systems as it used a mixed cosurfactant system of citronellol and ethanol to achieve BME formation. Campo et al., (2004) who previously used a W-IV with Tween 80, ethanol, limonene, glycerol, and water proposed the possibility of bicontinuous structured microemulsions when the aqueous phase was 30-60% of the system volume. The aqueous phase was composed of water and glycerol. Although there are studies on the addition of drugs to various microemulsion systems, fewer studies exist on the addition of AMPs and/or proteins to microemulsions. Furthermore, there are only a few studies on the addition of AMPs to BMEs, and not many that test the antimicrobial effects of these systems.

1.5.2 Microemulsions Systems to Encapsulate Proteins

Other studies described three common methods have been used to entrap proteins and peptides in reverse micelles (Anil and Kannan, 2018). The first method is injection, where an enzyme is made into a solution that is added to a surfactant solution and shaken until optically clear. The second method entraps a protein by adding a dry lyophilized protein to the surfactant-oil solution and is followed by the addition of an aqueous phase. The third method, used with a two-phase microemulsion, allows the protein to entrap spontaneously when the aqueous phase is added to the surfactant-oil phase (Anil and Kannan, 2018). This method can also be applied to formation of a W-III. Each of these methods have their own benefits and this project will follow the third approach by adding AMPs to the aqueous phase and adding that to the oil-surfactant mixture. Anil and Kannan (2018) also describe multiple systems currently used in research studies to incorporate proteins into microemulsions. These systems include self-emulsifying drug delivery systems (SEDDS), self-microemulsifying drug delivery system (SMEDDS), self-nano-emulsifying systems (SNEDDS), solid-lipid nanoparticles (SLN'S) and more. SEDDS are divided into sub-groups of SMEDDS and SNEEDs which are clear systems with a size range of 100 to 250 nm (SMEDDS) and <100 nm (SNEDDS). SNEDDS were researched mainly for oral delivery and showed protection and stabilization of encapsulated proteins. SLN's are advantageous because they are physically stable and allow for a controlled release a drug (Anil and Kannan, 2018).

1.5.3 Factors that Affect Protein Transfer

In order to understand the addition of AMPs into BMEs, background literature review was conducted on the encapsulation and extraction of proteins. Microemulsions have been used for protein extraction and encapsulation within each of the Winsor systems. Factors affecting protein transfer in relation to the aqueous phase include pH, ionic strength, and type of salt (Pires et al., 1996). Protein transfer is also dependent on properties of the protein which include isoelectric point, size and shape, hydrophobicity, and charge distribution (Pires et al., 1996).

Liquid-liquid extraction is an appropriate method for the isolation of a protein. It is defined as a method "for extracting a solute from a solvent solution in a certain solvent, by another solvent" (Berk, 2018). The liquids used in this extraction method are typically

immiscible or partially immiscible with one being an aqueous solution and the second being a non-polar organic liquid (Berk, 2018). The steps in liquid-liquid extraction include first mixing the liquid phases together then allowing the phases to separate (Berk, 2018). Microemulsions have been reported as a successful tool in isolating and extracting proteins. The factors affecting protein transfer are important when considering what components to use in a microemulsion system. Pires et al (1996) discuss five main factors that affect the transfer of proteins using liquid-liquid extraction: pH, ionic strength, type of electrolyte, surfactant concentration, and charge distribution. Typically, electrostatic interactions are the main driving force between proteins and surfactants that are anionic or cationic. The pH of the aqueous solution is significant because it affects the net charge of proteins. Extreme pH values are undesirable because they can lead to protein denaturation. The salinity concentration affects the ionic strength of the aqueous phase. When ionic strength is increased, it reduces the electrostatic interactions occurring between the protein and surfactants due to the Debye screening effect. To achieve the ideal protein transfer, the minimum value of ionic strength should be used. As surfactant concentration is increased, protein solubilization is positively affected. However, an increase in surfactant concentration results in a more difficult recovery of the protein. The charge distribution is significant because protein extraction yields are dependent on their charge. Pires et al (1996) discussed that in some cases, higher charges on proteins lead to more easily extracted proteins.

1.5.4 Microemulsion Protein Extraction Methods

Protein isolation and purification using W-II systems can be described in two main steps: forward and backward extraction. Forward extraction is the process of extracting the protein from an aqueous phase into the w/o microemulsion phase of a W-II system (Fig. 13). This occurs by adding the protein enriched aqueous solution to the surfactant oil mixture to create a W-II system. Following forward extraction is back extraction which is the process of removing and recovering the microemulsion-encapsulated protein into a new aqueous phase (Fig. 14). Back extraction typically occurs using an aqueous stripping solution to reduce the driving force of the surfactant and protein (Gomez del Rio and Hayes, 2011). Pires et al (1996), described two main methods as the driving forces in forward transfer: electrostatic interactions and hydrophobic interactions. For back extraction, researchers have used electrostatic repulsion of the surfactant
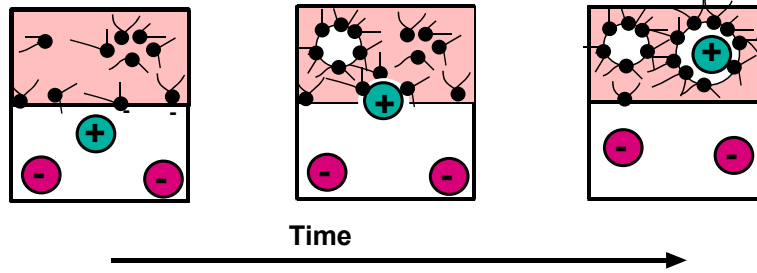
Figure 13. Forward extraction of a protein using a W-II microemulsion; black figures represent anionic surfactants, red phase represents oil, white phase represents an aqueous solution containing positive and negatively charged proteins (Hayes, 2012)
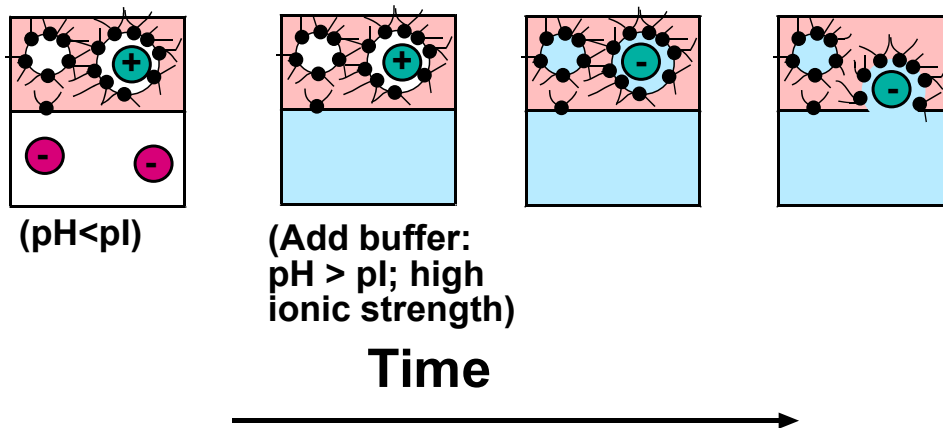
Figure 14. Back extraction of protein using a buffered solution with high ionic strength; red phase represents oil containing reversed micellar-encapsulated proteins formed via forward extraction (Figure 13), white phase is the aqueous solution, after the white phase is removed a stripping solution is added depicted in blue and used to recover the protein. The stripping solution is at a pH>pI of the protein, to induce a negative charge for the latter (Hayes, 2012)

and protein through pH or salinity increases of the aqueous phase. Although W-I and W-II microemulsions have been used to extract proteins, it has been reported that there was a decrease in yield from forward extraction when proteins were back extracted. A more recent study proposed a method using W-III systems for forward and backward extraction (Gomez del Rio and Hayes, 2011). Their study was successful in extracting proteins using W-III systems.

1.5.5 Bicontinuous Microemulsion Protein Extraction

Many studies were carried out using W-I and W-II systems for the delivery of proteins and peptides. However, in a study conducted by Gomez del Rio and Hayes (2011), a protein was successfully forward and back extracted to and from the middle phase of a W-III microemulsion (Fig. 15). In their study, their microemulsion systems consisted of isooctane, aerosol-OT (AOT), CK-2, 13 $E_{5.6}$, and NaCl solution. They tested these systems with the addition of four different proteins: α-chymotrypsin, cytochrome c, lysozyme, and bovine serum albumin (BSA). The first objective achieved with their microemulsion system was forward extraction of the protein to the middle phase. Forward extraction to the middle phase from the aqueous phase occurred because of electrostatic forces or hydrophobic interactions. This occurred by combining the protein enriched aqueous phase with the surfactant enriched oil phase. Once combined, the electrostatic forces between the proteins and the anionic surfactant caused the protein to partition into the middle (BME) phase of the W-III system. It was also found that hydrophobic interactions were an additional force that contributed to the extraction of BSA. Greater than 90% of the proteins to the middle phase through forward extraction was achieved. Following forward extraction was back extraction, a method used to recover the protein from the microemulsion system. Back extraction worked by removing the bottom layer of the W-III system and replacing it with an alkaline buffer or a highly concentrated NaCl solution with binary surfactant. Additionally, a small amount of surfactant/oil solution was added due to the increase of lipophilicity as a result of the change in salinity (Fig. 15). Using this method, the forces bonding the surfactant and protein together were negated, allowing for the release of the protein to the middle phase resulting in back extraction. This study showed a successful method in encapsulating proteins using W-III systems which can be explored for the encapsulation of AMPs.
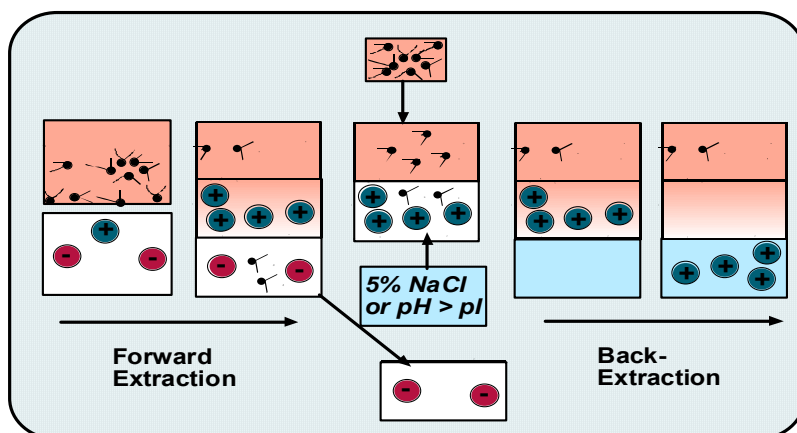
Figure 15. Diagram of forward and back-extraction of a protein from a W-III system using a stripping solution to release the surfactant bond to the protein. Red represents oil, black represents surfactant, blue plus signs represent a positively charge protein, red minus signs represent an anionic surfactant, and the blue represents an aqueous stripping solution (Hayes, 2012)

1.5.6 Melittin Encapsulation into Microemulsion and Characterization

Hayes et al., (2018) conducted a study on the encapsulation and characterization of melittin in W-III BME systems. Their goal was to evaluate the BME system's efficiency to encapsulate melittin into the middle bicontinuous phase in a bioactive conformation. They used 2 BME systems; the first used water/AOT/CK-2,13/heptane, and water/sodium dodecyl sulfate (SDS)/1-pentanol/dodecane. AOT and SDS are both anionic and were chosen to attract the positively charged melittin through electrostatic forces. The binary surfactant system, AOT/CK-2,13 was accurately formulated for each system. Another BME system with a nonionic surfactant was used to compare how melittin reacted to the nonionic surfactant and an anionic surfactant. Hayes, et al. (2018) successfully encapsulated melittin into their BME systems. They determined the melittin concentration in the middle phase using a spectrophotometric assay. The systems were characterized using circular dichroism, fluorescence spectroscopy, and small-angle neutron scattering. Results showed they extracted greater than 75% melittin to the middle phase of the W-III systems in concentrations from 1.5 to 5.3 g/L. The nonionic system was unsuccessful in extracting melittin to the middle phase. The BME systems showed a decreased in the middle phase volume as the concentration of melittin increased. Circular dichroism results showed melittin reflected a higher percentage of an alpha helical structure encapsulated in the BME compared to an aqueous solution. Fluorescence spectroscopy results showed a blue shift in melittin from and aqueous solution to a BME system. This meant melittin was residing within the surfactant monolayers environment within the BME. Hayes et al., (2018) were successful in encapsulating a model AMP, however, the materials used for their BME systems would not be suitable as a topical delivery system. Research is required to identify BME systems that consist of biocompatible materials and to determine antimicrobial effects, if any, of AMP loaded BMEs to treat bacteria commonly found in SSIs and chronic wounds.

1.6 Research Objective

It was hypothesized that because AMPs are typically cationic, electrostatic forces promoted by anionic surfactants will drive the partitioning of AMPs into BMEs. It was also hypothesized from preliminary research and literature review, that when encapsulated, AMPs will be in their most active state, leading to an effective treatment. This project aimed to identify

multiple bicontinuous microemulsion (BME) systems created with biocompatible materials to encapsulate AMPs in their most active state. This project also aimed to test the effectiveness of encapsulated AMPs on various strains of Gram-positive or Gram-negative bacteria associated with chronic wounds and SSIs by using antimicrobial diffusion techniques. The structures of the BMEs and the AMPs encapsulated in the BMEs were characterized using various molecular-level measurements which include small-angle x-ray scattering, circular dichroism, and fluorescence spectroscopy.

CHAPTER 2: METHODS FOR ANALYSIS OF AMP LOADED BMEs

2.1 Introduction

Due to the nanoscale sizes of AMPs and BMEs, nano-level characterization is required to confirm if the microemulsion systems created are bicontinuous in nature and if they successfully encapsulated AMP in a bioactive conformation. Nano-scale characterization is important to understand how the AMP and/or the BME structures are altered when encapsulated. Small angle x-ray scattering (SAXS) is commonly used to characterize the structure of microemulsions. Circular dichroism (CD) spectroscopy measurements characterize the secondary structure of proteins or peptides. Fluorescence spectroscopy is used to indicate the relative hydrophilicity or hydrophobicity of the environment where a protein or peptide's tryptophan residues reside within a solution. In addition to molecular characterization, antimicrobial assays are required to determine if AMP loaded BMEs inhibit bacterial growth compared to controls such as water and empty BMEs. Antimicrobial assays methods include dilution and diffusion. Chapter 2 focuses on an overview of the molecular methods that were used to test this project's melittin loaded BMEs. This chapter also summarizes background information on antimicrobial tests used in this research.

2.2 Nanoscale Characterization of BMEs

Since W-IV system are one phase, it is not easy to distinguish between what type of W-IV system is achieved when created. For this project, SAXS was used to confirm that BMEs were formed and to identify any structural changes to the BMEs due to the addition of an AMP. Another related method to characterize microemulsions is small-angle neutron scattering (SANS). This section describes and overview of SAXS, SANS, and the model used to fit scattering data for BMEs.

2.2.1 SAXS and SANS Overview

Small angle scattering (SAS) can be used with an incident beam of x-rays or neutrons to characterize matter on a nanoscale level (Svergun and Koch, 2003; Hammouda, 1995). x-ray scattering can be used to determine structures of lipids, fibrous materials, muscles, and viruses (Hukins, 1981). Both SAXS and SANS characterize metal alloys, emulsions, nanoparticles and more (Svergun and Koch, 2003). In the process of SAS, a source of x-rays or neutrons at a

specific wavelength and intensity, after its collimation, is shot at a sample of matter and the scattering intensity data is detected and collected for analysis. Figure 16 displays a schematic of the SANS process. The angle θ refers to the detector position relative to the incident beam of x-rays or neutrons (Fig. 16). The sample to detector distance can be modified to gather scattering data at different length scales. The scattering vector is defined as $Q=k_s-k_i$ (Hammouda, 1995). This vector is the magnitude and length of the scattering from the sample to the detector. Q is also defined as:

$$Q = 4\pi * \frac{\sin\left(\frac{\theta}{2}\right)}{\lambda} \tag{2}$$

where,
Q= scattering vector
θ= scattering angle
λ= wavelength.

Q is directly related to the angle θ and is representative of different length scales of the matter being measured. As the value of Q increases, the length scale of matter tested decreases. Although the scattering sources for SANS and SAXS differ, the same data reduction can be used for each. SAS data consists of I(Q) vs Q and is often analyzed by form factor-structure factor modeling:

$$I(Q) = N_p * V_p^2 * (\Delta\rho)^2 * P(Q) * S(Q) + B_{incoher} \tag{3}$$

where,

I(Q)= the scattered light relating to the scattering vector, scattering intensity
N_p= number concentration of scattering bodies
V_p= volume of scattering body
$\Delta\rho$= difference in scattering length density or contrast
P(Q)= the shape or form factor
S(Q)= interparticle structure factor
$B_{incoher}$ = the incoherent background signal.

P(Q) is the form or shape factor which measures the size, shape, and internal structure of a single particle of the matter measured. S(Q) is the interparticle structure factor which measures the interactions of the particles within the matter measured. The change in ρ refers to the differences in the scattering length densities of the components within the matter being tested. The scattering length density, ρ, defined:
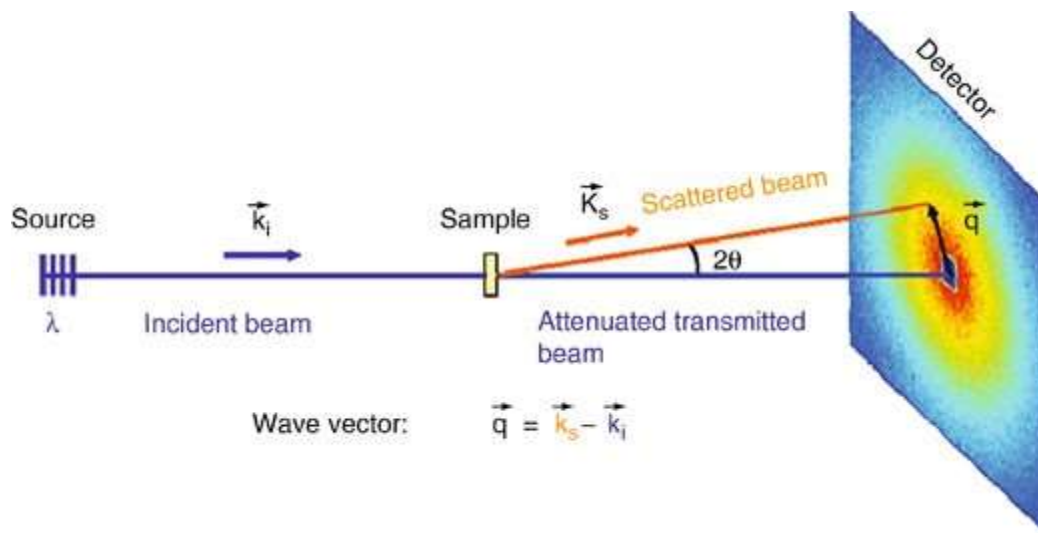
Figure 16. Diagram of neutron scattering where vector q is detected in the detector

$$\rho = \frac{1}{v_m} \sum_{i=l}^{N} b_i \tag{4}$$

where,

v_m= molecular volume

b_i= bond coherent scattering length of atom i.

Scattering length density is calculated for x-rays and neutrons based on their molecular formulas and density as inputs through on-line tools such as the National Institute of Standards and Technology (NIST) neutron activation and scattering calculator.

2.2.2 Difference of SAXS and SANS

Due to the differences between the scattering of neutrons and x-rays on a molecular level, significant differences exist between SANS and SAXS. SANS requires deuteration of one or more of the materials of the substances being tested because neutrons interact differently with deuterium and hydrogen. Deuteration is defined as the addition of deuterium to substance. This allows a researcher to add deuterium to a specific phase of the matter being tested in order to control the interface at which neutron contrast occurs. The scattering intensity of hydrogen is higher than the scattering intensity of deuterium (Hayes, 2015). Deuteration is not relevant for SAXS measurements. Scattering intensities also vary between SAXS and SANS for different molecules (Fig. 17). In Figure 17, the circles represent "scattering cross sections," which represent the scattered intensity I(Q). The larger circles represent a larger amount of scattering due to the interaction of the beam with the molecules. Substances with a larger density are more compact in their atomic and molecular density, which increases the extent of scattered intensity (Hayes, 2012). For SANS, larger scattering intensities occur for hydrogen when compared to SAXS. SAXS will have larger scattering intensities for heavy metals and oxygen when compared to SANS.

2.2.3 SAXS and SANS Analysis for BMEs

SAXS can be used to determine the structural changes of the BMEs due to the addition of a protein or peptide, a change of composition or a change of an environmental parameter. When x-rays interact with microemulsion components the scattering intensity is driven by the
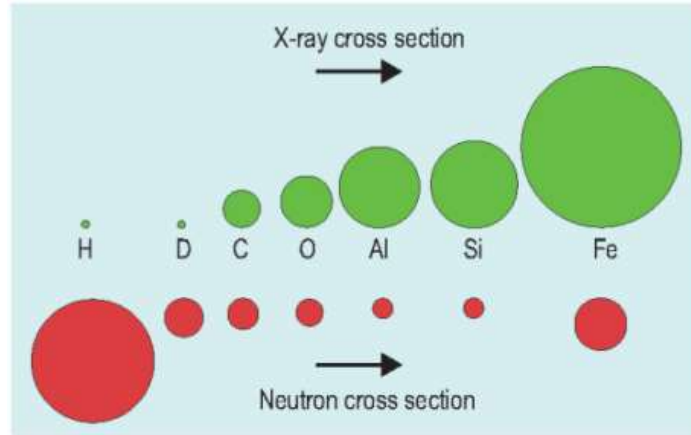
Figure 17. Cross sections of scattering for neutron and x-rays (Jacobson et al., 2004)

differences in the density of the microemulsion components. This data can be used to analyze the differences in microemulsion systems. SAXS and SANS data for BMEs are analyzed through fitting using the Teubner-Strey (T-S) model that is used specifically for BMEs (Teubner and Strey, 1987). An example of a T-S fitting of SANS data for BMEs is displayed in Figure 18. The T-S model consists of a bell-shaped curve. On a nanoscale level, the BME systems can be confirmed if they are bicontinuous or not based on the outputs from SAXS. Also shown in Figure 18, is a change in Q_{max}, the maximum Q value, for various concentrations of cytochrome c within the BME. Equation 1 in Figure 19 shows the T-S model. The T-S model determines the quasi-periodic repeat distance (d), correlation lengths (ξ), and amphiphilicity factor (f_a) of the BMEs (Fig. 19). The quasi-periodic repeat distance is defined as the average distance across the oil and water nanodomains of the bicontinuous phase, shown as value d in Figure 20. The correlation length represents the length associated with a certain number of surfactants residing together at the interface, where the surfactant molecules' motion is correlated represented by $1/\xi$ in Figure 20 (Hayes et al., 2014). The correlation length is inversely proportional to the surface area per volume of the surfactant monolayers (Hayes et al., 2014). The amphiphilicity factor represents a scale that described the degree of ordering the surfactants (Schubert and Strey, 1991).

2.3 Molecular Characterization of Proteins and Peptides

CD and fluorescence spectroscopies are methods to characterize proteins and peptides in the solutions they reside in. CD spectroscopy is used to determine the secondary structure of a protein within a solution. Fluorescence spectroscopy is used to determine the location of the protein residues within the solution they reside in. Fluorescent measurements provide information on the environment of the proteins within the sample being measured.

2.3.1 Circular Dichroism

CD is a spectroscopic method that measures differences of molecules within a system and how they interact with the absorption of left-handed and right-handed circularly polarized light
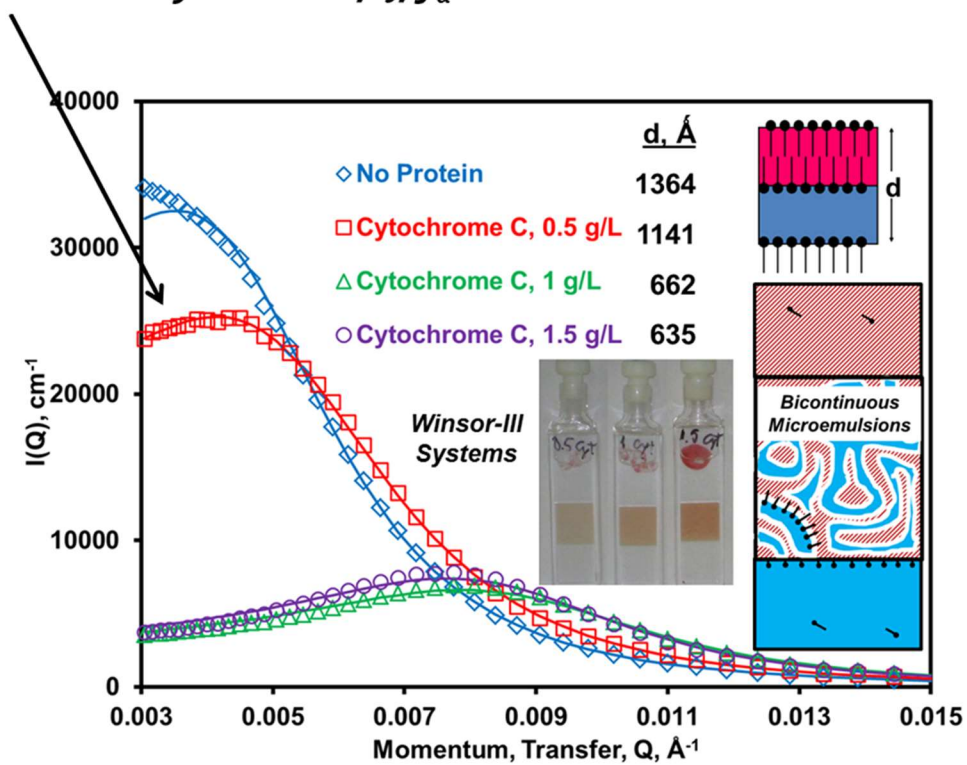
Figure 18. T-S fitting for BMEs containing varying concentrations of cytochrome c (Hayes et al., 2015)

$$I(Q) = \frac{1}{a_2 + c_1 Q^2 + c_2 Q^4} + bkgrnd$$

$$d = \frac{2\pi}{\sqrt{\frac{1}{2}\sqrt{\frac{a_2}{c_2}} - \frac{c_1}{4c_2}}}$$

$$\xi = \frac{1}{\sqrt{\frac{1}{2}\sqrt{\frac{a_2}{c_2}} + \frac{c_1}{4c_2}}}$$

Figure 19. Teubner-Strey model equations: I(Q) is the T-S function of scattering intensity, *d* is the quasi-periodic repeat distance, and ξ is the correlation length
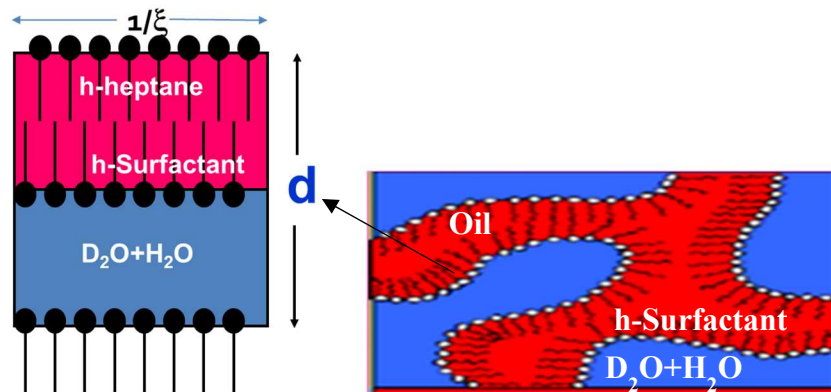
Figure 20. Oil and water nanodomains of a BME: Oil represented by the red, water represented by the blue, and surfactant by the black. The quasi-periodic repeat distance is shown as *d* and the correlation length is shown as 1/ξ (Hayes, 2015)

(Woody, 1995; Greenfield, 2007). The use of circularly polarized light, which is chiral, allows for the accurate measurement of the secondary structure of most biological molecules (Woody, 1995). Distinct spectra will vary for different polypeptide structures such as α-helix, beta-sheet, or random coil. CD spectra measurements are carried out in a spectrometer. Samples are placed on high-transparency quartz cuvettes that can be rectangular or cylindrical in shape. Pathlength cells can vary in sizes from 0.01-1 cm (Woody, 1995).

CD measures ellipticity to determine the secondary structure of proteins and peptides (Greenfield, 2007). Plots of CD data may determine the structure of a protein by comparing it to common spectra of structures such as α-helix, beta-sheet, and random coil (Fig. 21). Protein structures can be determined by taking measurements from 190-230 nm. It is typical for an alpha-helical protein to have two minima at 208 and 222 nm and a strong maximum at 191 nm (Wei et al., 2014). Beta-sheet contains a minimum at 215 nm and a maximum at 198 nm (Fig. 21). CD spectra readings can prove to be useful in determining the secondary structure of an AMP within a BME. This method has been used in previous research to determine the structure of melittin in BMEs (Hayes et. al., 2018).

2.3.3 Fluorescence Spectroscopy

Fluorescence spectroscopy can be used to determine protein folding and membrane proteins environments (Ladokhin, 2000). This method works by detecting changes in the environment of the fluorophore within a protein (Ladokhin, 2000). Fluorescence intensity is measured over a wavelength and kinetic time. Proteins interact with fluorescence excitation due to their tryptophan residues. Ladokhin, (2000) stated the fluorescence of, "tryptophan residues in proteins varies from 307 to 353 nm." Fluorescence emission spectra are used to determine the characteristics of the environment the protein or peptide resides within. Fluorescence spectroscopy measurements can be taken using quartz cells or well plates. A high-energy continuum light source is excited to a desired wavelength, passed through a monochromator, and enters the sample to be measured (Senesi and D'Orzaio, 2005). Wavelengths are detected and recorded for analysis.

Fluorescence measurements for this project, are used to infer the location of melittin within the BMEs. Fluorescence readings can indicate if there is a shift in the spectra maxima. A
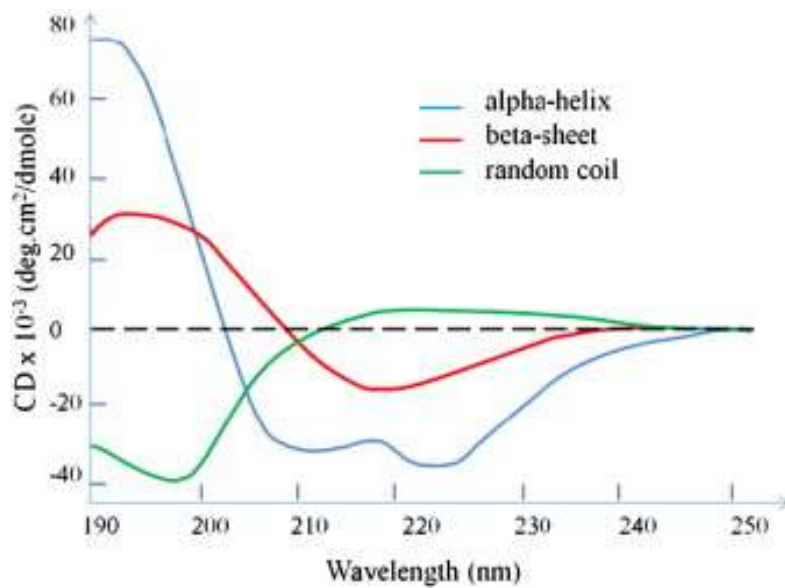
Figure 21. CD spectra for alpha-helix, beta-sheet, and random coil protein structures (Wei. Et al., 2014)

blue shift in fluorescence occurs when the maximum of fluorescence graphs shifts to the left on the x-axis. This indicates the protein or peptide has moved to a more apolar environment when compared to the initial solution the protein or peptide resided within. For these experiments, the initial solution refers to an aqueous solution that mimics the aqueous phase of the BMEs in terms of salinity and pH. If a blue shift occurs for melittin encapsulated in BMEs, this likely means the AMP resides within the surfactant monolayers.

2.4 Antimicrobial Susceptibility Testing

There are a few methods commonly used to test for bacterial susceptibility to treatments. The main susceptibility tests include diffusion assays and broth dilution and plating also known as minimum inhibitory concentration (MIC) testing. (Fig. 22) (Tenover, 2017). Diffusion assays test the ability of a treatment to diffuse through the agar and prohibit or inhibit bacterial growth (Fig. 24). Broth dilution and plating are used to determine MIC, which is the minimum concentration of treatment required to inhibit bacterial growth. Antimicrobial assays are completed aseptically under a biological hazard hood or under a flame to minimize sample contamination. All materials for antimicrobial assays are required to be autoclaved before use.

Disk diffusion tests the ability of a treatment to inhibit bacterial growth with paper disks that are pretreated, or treatment is added. Disk diffusion occurs by placing pre-made disks with selected treatments onto a lawn of bacteria contained on an agar plate, then allowing the system to incubate, and checking the agar plate for a zone of inhibition (Tenover, 2017) (Fig. 23). A zone of inhibition is defined as the area around the treatment disk location that inhibited bacterial growth on the lawn. To create a lawn of bacteria a spreader or swab can be used. In this project, a spreader was used. A volume of overnight bacteria culture is washed in a saline buffered solution prior to making the lawn of bacteria. The lawn of bacteria is created by spread plating a determined volume of washed bacteria culture onto a chosen agar medium. This is followed by the addition of the treated paper disks to the surface of the agar on top of the lawn of bacteria. Plates are incubated overnight, then removed from the incubate and zones of inhibition are measured. Typically, two perpendicular measurements are taken of the diameter zones and averaged for each zone. Well-diffusion is another diffusion assay. The same set up as disk
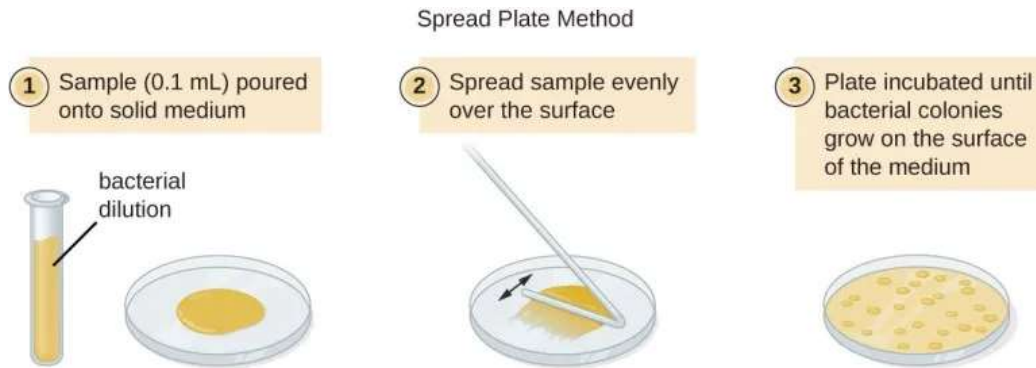
Figure 22. Example of the spread plate method that is used in dilution plating and/or lawn creation for diffusion assays (Rijal, 2022)
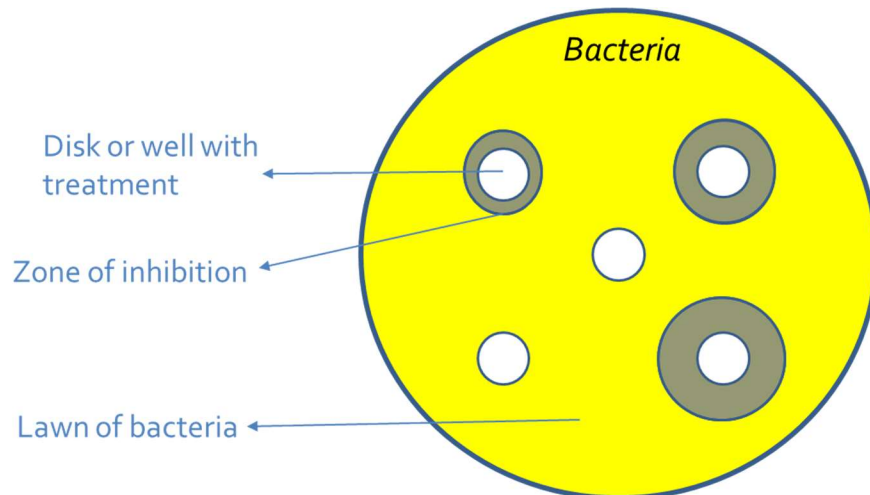
Figure 23. Example of a disk diffusion set up, yellow represents the lawn of bacteria, white circles represent disks, and grey circles represent zones of inhibition

diffusion is used, except wells are bored within the lawn of bacteria on agar for treatment to be placed within. A set volume of treatment is added to each of the wells and the plates are incubated for 24 hours. After 24 hours the zones of inhibition are measured and compared to controls: system with no antibiotics and also known antibiotics, the latter of which serves as a positive control.

MIC testing is grouped into agar and broth dilution methods. This method produces a precise quantitative result for antimicrobial susceptibility. Broth dilutions are completed in well plates. Well plates consist of multiple wells that can be loaded with the chosen treatment. Components that are added to a well include nutrient media, bacteria culture, saline solution, and treatment. Once the components to the well-plate are added, they are placed read in a well plate reader for 24 hours. A well-plate reader measures optical density to determine the bacterial growth kinetics of each well. If the treatment is effective, the observed bacterial growth should be minimal. This is further tested by diluting and plating the components from a well plate. Components from the well plate are added to a buffered saline solution. Then serial dilutions occur to dilute the bacterial concentration. A volume from these dilutions is added to agar and spread plated with a spreader (Fig. 23). Plates are left to incubate for 24 h; then bacterial counts are measured. Any count above 200 is considered too many to count (TMTC) and is to be disregarded. Agar dilution occurs by creating agar containing the treatment to be tested at different concentrations. Bacterial cultures are added to the plates in different concentrations and incubated for up to 16-18 hr for non-fastidious organisms and 18-24 hr for fastidious organisms, or organisms requiring complex nutrition (Tenover, 2017).

2.5 Conclusions

SAXS, CD, and fluorescence have been successful in characterizing microemulsions, peptides, and proteins previously which were described in this chapter. For this project, SAXS was used to characterize melittin loaded BME systems. CD spectroscopy was used to determine the secondary structure of melittin in the BMEs compared to an aqueous solution. Fluorescence spectroscopy was used to determine the location melittin resided in within the BMEs. Some studies have used antimicrobial assays with microemulsions (Jantrawut et al., 2018; Viyoch et

al., 2006). However, these studies did not focus on BMEs. This project tested dilution and diffusion assays with melittin loaded BMEs.

CHAPTER 3: RESEARCH CONDUCTED

3.1 Introduction

As described in Chapter 1, SSIs and chronic wounds require new treatments to combat the rise in antibiotic-resistant microorganisms. A possible solution to treat bacteria commonly found in wounds and infections is to use AMPs. AMPs disrupt cell membranes and are not designed to target any specific bacteria. Although never impossible, there is a less likely chance of bacteria becoming resistant to AMPs. Some studies have attempted to produce an effective AMP treatment; however, many were unsuccessful due to unfolding, stabilization, cytotoxicity, and effectiveness issues (see section 1.3). New and effective delivery systems for AMPs are required to combat the rise in antibiotic resistant microorganisms. BMEs are a potential robust delivery system because their elongated nanodomains mimic bio-membranes which would serve to encapsulate AMPs. Previous research was successful in encapsulating the AMP, melittin, however the microemulsions in that study were created with alkane oils which are not biocompatible. The objective of this chapter was to identify candidate BMEs created with biocompatible materials. Once systems were identified, the goal was to determine if melittin, a model AMP, can be solubilized in BMEs in an active conformation. To complete this goal the change in structure of the melittin loaded BMEs was characterized using SAXS. The characterization of melittin was completed using CD and the environment of the melittin within the BMEs was characterized using fluorescence spectroscopy. Finally, this project had the goal of determining antimicrobial effects of the AMP loaded BMEs using antimicrobial assays.

3.2 Materials

AOT ($\geq$97% pure), Polysorbate 80 (Tween 80), Polysorbate 85 (Tween 85), sodium oleate, sorbitan monooleate (Span® 80), lecithin, sodium caprylate ($\geq$99% pure), beta-citronellol (95% pure), ©-(+)-limonene (97% pure), and melittin from bee venom ($\geq$85% HPLC) a + 6-charged peptide, octanoic acid (caprylic acid +98% pure), IPM ($\geq$ 98% pure), and Cytochrome c from horse heart (dialyzed and lyophilized; MW = 12 kDa, pI=2.2-3.0) were purchased from Sigma-Aldrich (Milwaukee, WI, USA). Ethanol and 1-propanol (certified), polystyrene 96 well plates and Falcon™ 96-well, non-treated, U-shaped bottom polypropylene plates, Tryptic soy broth (TSB), tryptic soy agar (TSA), phosphate buffered saline (PBS), Mueller Hinton agar

(MHA), Noble agar, blank paper disks, ciprofloxacin disks, and gentamicin antibiotic liquid were purchased from Fisher Scientific (Pittsburgh, PA, USA).. Frozen bacteria cultures were (See Table 2) were aseptically transferred to TSB and incubated for 24 h at 37°C thrice and also streaked for isolation on TSA and isolated colonies were transferred to TSB. Mark-tubes made of Quartzglass, 0.1 mm wall thickness were purchased from charlessupper company (Westborough, MA, USA).

3.3 Methods

3.3.1 Preparing Microemulsion Solutions

BME systems were created at room temperature $23\pm1°$C that was measured each day. Each BME system was created by solubilizing the surfactant components into the oil phase first and vortexed until fully combined. This was followed by the addition of the aqueous phase to the oil surfactant mixture. The aqueous phase was either water only or water with NaCl. A pH buffer of 5 mM was created using dibasic and monobasic phosphate salts as an additional control parameter for the aqueous solution. This insured each system was created with the same pH that averaged 6.95 for water only and 6.80 for the 85 mM NaCl solution. Aqueous solutions were tested using a pH meter to confirm they were at the correct pH. Some systems were placed in an incubator set to $30°$C to aid in dissolving the surfactants into the oil mixtures. The components for each system are found in Table 4. This includes their weight percentages overall for each component.

3.3.1.1 System 1: AOT/Tween 85 System

System 1 was created using anionic surfactant AOT, nonionic surfactant Tween 85, IPM, and water (Table 4). The aqueous solution was varied with and without NaCl for the systems. The surfactant ratio of AOT:Tween85 was 2:1 w/w, was kept the same for each of the systems. The water: oil ratio was 0.6:1 w/w for systems 1A and 1B and 1:1 w/w for system 1C. System 1A was created using surfactant concentrations for the overall microemulsion of 15-20%. System 1B was created with surfactant concentrations for the overall microemulsion between 11-13%. System 1C was created with surfactant concentrations for the overall microemulsion between 3-5%. Multiple salinity concentrations were tested to obtain a W-III system with these components

Table 4. Components in candidate bicontinuous microemulsion systems

System #	Winsor-Type	Surfactant(s)	Surfactant w%,	Cosurfactants	Cosurfactant w%	Oil	Oil w%	Aqueous Solution	Aqueous w%	Temp. (°C)	Ref.
1A	IV	AOT, Tween 85	13.3, 6.7	-	-	IPM	50	pH buffered water	30	23	
1B	III	AOT, Tween 85		-	-	IPM		pH buffered water		23	(Liu et al., 2009)
1C	III	AOT, Tween 85	3.3, 1.7	-	-	IPM	47.5	85 mM NaCl	47.5	23	(Yanyu et al., 2012)
2	IV	Sodium oleate	15	Citronellol, ethanol	1.12, 13.8	Limonene	20	pH buffered water	50	23	(Klossek et al., 2012)
3	III	Sorbitan monooleate, lecithin, sodium caprylate, caprylic acid	3.6, 1.2, 2.5, 0.9	-	-	IPM	46.4	150 mM NaCl	45.4	23	(Tamhane et al., 2012)
4	IV	Tween 80	21.4	Ethanol	21.4	Limonene	7.15	pH buffered water, glycerol	39.5, 10.4	23	(de Campo et al., 2004)
5	IV	Lecithin	19	1-propanol	19	Limonene	57	pH buffered water	5	23	(Corswant and Thoren, 1999)

pH was 6.95 for water only and 6.80 for 85 mM NaCl

AOT= Aerosol-OT, IPM= Isopropyl myristate,

at a lower concentration than the W-IV system. Salinity was tested from 50 mM to 150 mM, and a salinity of 85 mM was chosen as the optimal salinity for system 1C.

3.3.1.2 System 2: Sodium Oleate System

The weight percentages used for system 2 were 15/1.12/13.8/20/50 sodium oleate/citronellol/ethanol/limonene/water. Sodium oleate was added to the citronellol, ethanol, and limonene and vortexed until fully combined. In the last step, water was added and mixed until a W-IV system was created.

3.3.1.3 System 3: Lecithin System

The components for this system were sorbitan monooleate, lecithin, sodium caprylate, caprylic acid, 0.9% NaCl solution, and IPM. A study was conducted using these components to determine what microemulsions would be created using different weight percentages of sodium caprylate (Yuan et al., 2008).

3.3.1.4 System 4: Tween 80/Ethanol System

The components of system 4 included nonionic surfactant Tween 80, glycerol, water, limonene, and ethanol. The aqueous phase was considered as glycerol and water combined. Systems were created with aqueous phases of 30, 40, 50, and 60%, each having a 3:1 w/w ratio of water to glycerol. Additionally, the ratio of Tween 80 to limonene was kept at 3:1 w/w for each system.

3.3.1.5 System 5: Lecithin/1-propanol System

System 5 included lecithin, 1-propanol, water, and limonene. BMEs were created with ratios of lecithin/1-propanol/water/limonene 19/19/5/57 w/w/w/w. Systems were created by combining lecithin with 1-propanol and limonene and vortexed until the lecithin was fully incorporated. Water was added to the mixed components and 1-phase system was created.

3.3.1.6 Cytochrome c Addition to Systems

Cytochrome c was added to the BME systems to visually determine if it would be accepted into the BMEs. The process included creating a 1.0 g/L concentration of cytochrome c in the appropriate aqueous solution and adding this solution to the surfactant oil mixture for each system: 1A, 1B, 1C, 2, 3, 4, and 5. Systems were visually observed, to determine if there were any phase changes and if the protein was accepted into the system.

3.3.1.7 Melittin Addition to Microemulsion Systems

Melittin was added to systems 1A, 1C, 2, and 4 using the same process as the addition of cytochrome c. Melittin stocks were created in the appropriate aqueous solution with concentrations ranging from 0.5-2.0 g/L and added to each of the BMEs. Systems 1A, 1C, and 4 accepted melittin into the BME phases.

3.3.2 Percentage of Melittin Extracted to the Middle Phase of System 1C

Bradford's assay was used to determine the percentage of melittin extracted to the W-III middle (BME) phase of system 1C. This assay was a colorimetric assay that uses Coomassie blue dye and spectroscopy measurements to determine protein concentration within a solution (Thermo Fisher Scientific Inc, 2017). A standardized graph was created by instructions given in the Bradford's assay kit for bovine serum albumin. A volume of 50 µL was extracted from the bottom aqueous phase of the W-III system and washed by centrifuge in 1000 µL of acetone. Once a protein pellet formed, the acetone was dumped, and the residual peptide was rehydrated with 50 µL of the appropriate aqueous solution. The rehydrated peptide was added to the Coomassie blue dye and photometric measurements were taken using a UV-Vis machine. Data collected from the melittin measurements were compared to the standardized graph. A concentration of melittin was calculated for the aqueous solution. The oil phase was washed with acetone, but residual peptide was not present. It was assumed that the melittin resided within the aqueous and middle phase of system 1C only. Mass balances were used to determine the concentration of melittin in the middle phase using the aqueous excess phase concentration and volume fraction of the W-III phases as inputs. Volume fractions were calculated for each phase

by measuring the height of each phase to the nearest mm and using the known inner diameter of the glass vials which was 5 mm.

3.3.3 SAXS Measurements and Analysis

SAXS measurements were carried out at room temperature, 23º C, on a Xenocs Xeuss 3.0 instrument equipped with D2+ MetalJet x-ray source (Ga Ka, 9.2 keV, wavelength [λ] = 1.341 Å). Measurements were collected at Oak Ridge National Laboratory (ORNL) in Oak Ridge, Tennessee. The instrument measured a Q range of 0.01 to 0.7 Å^{-1}. SAXS was used to measure BME samples with and without melittin at concentrations of 1.0 and 2.0 g/L for systems 1A, 1C, 2, and 4. A volume of 100 µL of a BME sample was added to a 0.1 mm quartz capillary tube and sealed with epoxy resin. The tubes were placed vertically in the sample holder and aligned perpendicularly to the directions of the x-ray beam in transmission mode.

SAXS data was analyzed using the T-S model commonly used for BMEs. The model aids in determining the quasi-periodic repeat distance (d), the correlation length (ξ), and the amphiphilicity factor (f_a). Data analysis was conducted using the software written by NIST staff scientists, that uses Igor Pro (v.5.0.4.7, WaveMetrics, Lake Oswego, OR) as a platform (Kline, 2006).

3.3.4 CD Spectroscopy

CD measurements were taken at room temperature at ORNL in Oak Ridge, Tennessee, using a JASCO J-810 spectropolarimeter to determine the structure of melittin within system 1C. Measurements of the W-IV systems were attempted; however, the high concentrations of surfactant caused the CD outputs to be noisy. Therefore, measurements were only gathered for system 1C. Similar to a previous study, a 0.1 mm pathlength cell was used to measure the wavelength of the system from 180-250 nm at 100 nm/min, with a bandwidth of 1 nm, data pitch of 0.5 nm, and 10 accumulations (Hayes et al, 2018). Measurements were taken for system 1C created with concentrations of 0.5, 1.0, and 2.0 g/L of melittin. For each BME measurement, 40 µL was extracted from the middle phase of the system and added to the 0.1 mm pathlength cell. An 85 mM aqueous solution with 2.0 g/L of melittin was also measured for comparison. For data

analysis, data collected for microemulsion without melittin was subtracted from the data with melittin. Two replicates of each sample were averaged and plotted for comparison.

3.3.5 Fluorescence Spectroscopy

Fluorescent spectroscopy measurements were taken at room temperature using a SpectraMax i3 microplate reader in Oak Ridge, Tennessee at ORNL. Systems 1A, 1C, and 4 were prepared with 0, 1.0, and 2.0 g/L of melittin. Three aqueous solutions that mimicked aqueous subphases of BMEs were prepared: (1) water only, (2) 85 mM NaCl, (3) water and glycerol mixture. For measurements, a 96 well plate was used in order to measure multiple samples easily. The well plate consisted of adding 100 µL of each microemulsion or aqueous solution in triplicate into the clear polypropylene 96 well plate. Samples were excited at 285 nm and the absorbance was measured across a wavelength of 310-450 nm at 2 nm intervals. The triplicate data collected for each system was averaged and corrected by subtracting the spectra of the BMEs without melittin from the BMEs with melittin. Data for each system and their respective aqueous solution were graphed for comparison.

3.3.6 Antimicrobial Assay Methods

Multiple antimicrobial assays were used to test the effectiveness of the melittin loaded BMEs. Dilution method with plating, disk diffusion, and well diffusion were the three methods attempted. Each method was conducted under a hood or under a flame to ensure no contamination to the samples. Each experiment was conducted at room temperature and if incubated, the temperature was 37° C. All materials were autoclaved (121° C) before use to ensure there was no contamination from the materials to the samples measured. Agar and growth media were prepared and autoclaved according to the manufacturer's guidelines.

3.3.6.1 Dilution, Plating, and Optical Density Measurements

Bacteria was grown in TSB and transferred to fresh TSB 24 hours before use in the well plates. In preparation for the 96-well plates, 1000 µL of bacteria culture was washed in 1000 µL of PBS. The 1000 µL of bacteria suspended in PBS was diluted 1:100 fold in PBS and used in

the well plates. TSA was also made according to manufacturing guidelines in preparation for plating and bacteria counts.

OD measurements of 96-well plates were taken using a Synergy HT well-plate reader (Winooski, VT USA) at 37º C. These plates consisted of 96 wells that held 300 µL of solution each. Added to each well was 40 µL TSB, 140 µL treatment or microemulsion component, and 20 µL bacteria suspended in PBS. The plates were placed in the well plate reader set at 37ºC for 24 hours with measurements taken at 600 nm every 10 minutes. Before each measurement, the well plate was shaken for 10 s at medium speed. Data produced from the measurements were used to graph growth kinetics of each well.

For plating, at hour 0 the 200 µL well components were added to 9ml PBS and used in a serial dilution. The solution was diluted in PBS to -2, -3, and -4 log dilution and a100 µL volume was taken from each tube and spread plated on TSA in duplicates. These plates were left in an incubator set at 37ºC and after 24 hours the bacteria number was counted and recorded. When the well plate reader was complete, the same dilution and plating process was conducted using the media from the wells. Components from a well were taken and added to PBS and diluted. If there was a treatment added to the well plate, less dilutions were done to determine the bacterial reduction. Wells without treatment had more dilutions completed to determine the bacterial growth. Once diluted, 100 µL were plated on TSA and left in an incubator set to 37º C for 24 hours. After 24 hours, the bacteria number was counted, recorded, and compared to the count from hour 0. Graphs from the 96 well plate reader were used as an indicator of growth or growth inhibition.

3.3.6.2 Diffusion Assays

All diffusion assays were performed under a flame under aseptic conditions. The first set of experiments with disk and well diffusion used TSA plates. TSA plates were created according to the manufacture guidelines and 20 mL were poured into petri plates. After issues with this media occurred, an attempt was made to create media with less gelatin to allow for better diffusion. Agar plates were created using M9 salts and Noble agar. However, the new agar would rip when spread plating was attempted. After initial testing, it was decided to attempt using another media, MHA.

Bacteria testing in disk and well diffusion include *S. aureus, E. coli* K-12, *E. faecium, P. aeruginosa, A. baumannii,* and *S. pyogenes.* Both disk diffusion and well diffusion assays used the same set up for lawn preparation. MHA plates of 15 mL were prepared according to the manufacturer's guidelines. Bacteria cultures were transferred to fresh TSB 24 hr before an experiment. A volume of 1000 µL of overnight bacteria culture for each bacterium was washed and added to 2000 µL of PBS. Lawns were prepared by spread plating 100 µL of the washed bacteria culture using a metal spreader. The metal spreader was dipped in ethanol and flamed before each use. Plates containing lawns of bacteria were created in triplicate for each system being tested.

Systems 1A, 1C, and 4 were created with 0, 1.0 and 2.0 g/L of melittin. For disk diffusion, disks were prepared by adding 30 µL of each treatment to a blank disk. Water (30 µL) was added to blank disks as a control. Disks with ciprofloxacin, a common antibiotic, were used as a positive control. Prepared disks were added to the surface of the agar using sterilized forceps. Each plate contained a water disk, antibiotic disk, melittin in aqueous solution varying in concentration disks, and melittin in BMEs varying in different concentration disks. Once the disks were placed on the surface of the bacteria lawns, they were left to rest for 15 minutes before placed in the incubator. The plates were left to incubate at 37° C for 24 hr. At hour 24 plates were checked for zones of inhibition. Zones of inhibition were measured using a ruler to the nearest mm. Two perpendicular diameter measurements were taken and averaged for each zone.

Well diffusion experiments were completed in triplicate for each bacterium. For well diffusion, after a lawn of bacteria was created, wells were bored from the agar using the back of a sterilized pipette tip. The wells were 5 mm in diameter and 60 µL of treatment were added to each well. Similar to disk diffusion, plates varied by treatment type. Water and 50% diluted gentamicin were used as controls. Lawns for each bacterium were created in triplicate for each treatment. Each plate included a well with water, diluted gentamicin, BMEs with varying concentrations of melittin, and aqueous solutions with varying concentrations of melittin. After treatments were added to the plates, they were left to sit for 10 min before placed in the incubator for 24 hr at 37° C. After 24 h, plates were checked for zones of inhibition around the wells. Zones were measured using a ruler to the nearest mm. Two perpendicular measurements were taken

and averaged for each zone. The diameters of the zones were corrected by subtracting the diameter of the wells. Diffusion assays were analyzed using statistical analysis. Statistical analysis comparison tests were completed using JMP, Version 16. SAS Institute Inc., Cary, NC, 1989-2021.

3.4 Results

3.4.1 Identified Microemulsion Systems

In this project, multiple biocompatible BME systems were identified (Table 4). The systems were created based on previous studied described in the literature (Liu et al., 2009; Yanyu et al., 2012; Klossek et al., 2012; Tamhan et al., 2012; de Campo et al., 2004; Corswant and Thoren, 1999). Additionally, cytochrome c, a membrane associated protein, and a model AMP, melittin, was successfully encapsulated into the systems. Systems were characterized at ORNL using SAXS, CD, and fluorescence spectroscopy.

3.4.1.1 System 1: AOT/Tween 85 System

System 1A was a W-IV system that formed within a minute of adding the components together. System 1B created a W-III system that fully equilibrated within 2 weeks (Fig. 24). It was determined that 85 mM NaCl aqueous solution formed an optimal W-III system for system 1C. System 1C created a W-III system in 15 minutes from mixing the components together (Fig. 25). It was found that each of these systems, especially 1A and 1C, equilibrated the best when kept at 30° C; however, they were able to equilibrate at room temperature, 23° C.

3.4.1.2 System 2: Sodium Oleate System

Some difficulties occurred with the addition of sodium oleate because there was a large amount of surfactant, specifically sodium oleate, required. Therefore, it took a while to fully combine. The system did combine and create a W-IV system (Fig. 26).
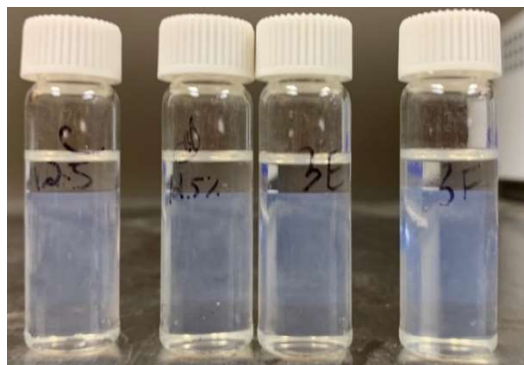
Figure 24. System 1B, W-III using 12.5% surfactant concentration
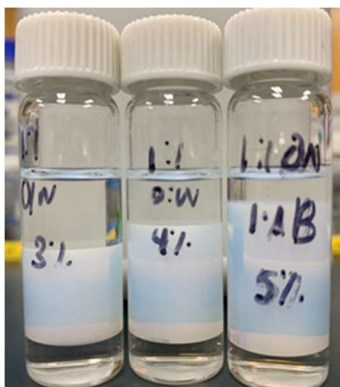
Figure 25. System 1C, W-III using 3, 4, and 5% surfactant concentration and 0.1M NaCl solution
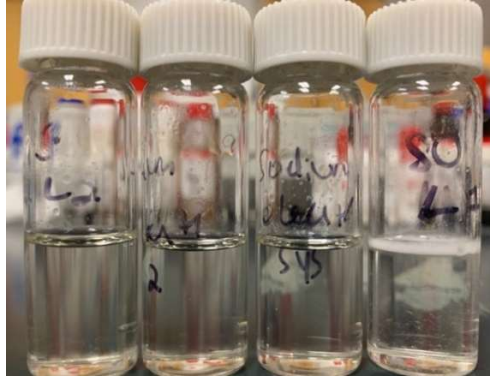
Figure 26. System 2 in 4 variations, starting left to right: the first is a w/o W-IV system, second and third are bicontinuous W-IV systems, and the fourth is a o/w W-IV system

3.4.1.3 System 3: Lecithin System

From the sodium caprylate scan, it was found that at 2.5% sodium caprylate, circled in red in Figure 27, there was a possible W-III system formed. These systems took roughly 2 weeks to equilibrate.

3.4.1.4 System 4: Tween 80/Ethanol System

When all components were combined, each system quickly formed a one phase solution (Fig. 28). This project chose to use the system with 50% aqueous phase to allow for an equal balance between the oil and water phases within the system.

3.4.1.5 System 5: Lecithin/1-propanol System

This system formed quickly once the lecithin fully dissolved. The W-IV system created was yellow in color (Fig. 29).

3.4.2 Cytochrome c Addition to Systems

Cytochrome c is a membrane protein that is positively charged and significantly less expensive than an AMP. This served as a control to give a better understanding if an AMP would be accepted into the BMEs. The bright red color of cytochrome c aided in the visualization of where the protein moved to when added to each system. Each system successfully encapsulated cytochrome c. System 1A showed a pink color throughout when cytochrome c was added (Fig. 30). In system 1C, the pink color was seen in the middle phase (Fig. 31). Figure 31 shows the difference in color between a system with and without cytochrome c. Cytochrome c was also added to systems 2, 3, 4, and 5. It was a little more difficult to visually see if it was accepted evenly throughout the system because there is only one phase. However, it can be hypothesized because they are W-IV systems, the cytochrome c would be evenly distributed throughout the one phase solution (Fig. 32). The addition of cytochrome c did not interfere with the quick formation of the W-IV solutions.

Figure 27. Samples of sodium caprylate scan on system 3 starting with 0.5% on the left and ending with 7% on the right. The red box highlights the system created with 2.5% sodium caprylate
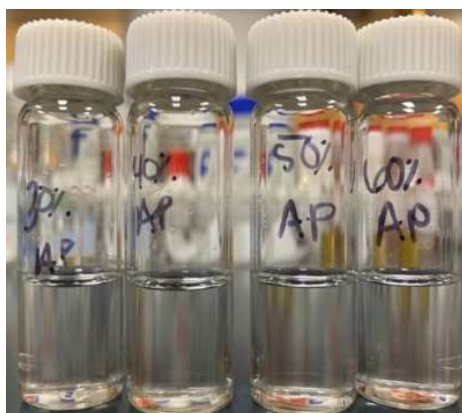
Figure 28. System 4 from left to right the aqueous phase varies in weight percentage of 30, 40, 50, and 60%

Figure 29. Two samples of system 5 that are clear yellow in color
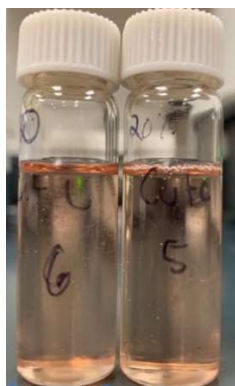
Figure 30. Addition of 1.0 g/L cytochrome c to system 1A, W-IV microemulsion

Figure 31. System 1C with cytochrome c in concentrations of 0.5 g/L (left group), 1.0 g/L (middle group), and 2.0 g/L (right group)
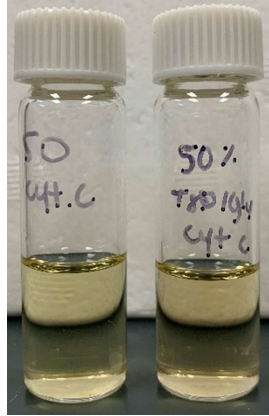
Figure 32. Cytochrome c addition to BME systems, on the left is system 2 and on the right is system 4

3.4.3 Melittin Addition to Microemulsion Systems

Melittin was accepted into systems 1A, 1C, 2, and 4 in concentrations of 0-2.0 g/L (Fig. 33). There were no obvious phase changes to the W-IV systems with the addition of melittin. For system 1C, the middle phase reduced in volume fraction as the concentration of melittin increased (Fig. 34). Column 3 in Table 5 shows the percentage the middle phase makes up of the three-phase system (System 1 C). Columns 4 and 5 show the percentages of water and oil within that middle phase. As the concentration of melittin increased, the volume of the middle phase decreased. There was also a more significant decrease in the percentage of oil accepted in the middle phase compared to the water accepted into the middle phase.

3.4.4 SAXS

Figure 35 shows the Teubner-Strey model fit to the SAXS data for system 1A and 1C. The model, commonly used for BME small-angle scattering data, describes a bell shaped relationship between Q and I(Q). The good fit of the T-S model to the SAXS data confirms that the microemulsions were bicontinuous in nature. A secondary scattering peak occurred near 2 Q_{max} for all BME samples, where Q_{max} is the Q position corresponding to the peak of the main scattering peak. The secondary peak likely represents multiple coherent scattering. Therefore, the secondary scattering peak was excluded when the T-S model was fit to the SAXS data (Silas and Kaler, 2003; Hayes et al., 2015). Correlation lengths and quasi-periodic repeat distances were calculated for each systema and displayed in Table 6. According to Table 6 as the melittin concentration increased, the quasi-periodic repeat distance decreased. The correlation length also decreased with an increase in melittin. The largest decrease was seen for system 1C. For system 1C, melittin caused a decrease in the surface activity of AOT because of electrostatic attraction and possible ion pairing between melittin and the sulfosuccinate group of AOT (Fig. 34). This resulted in a lower amount of water and oil solubilized to the middle BME phase. Further, because the correlation length is inversely proportional to the surface area per volume of BME phase there was a decrease in correlation length.

SAXS outputs for system 2 were different from system 1A and 1C. A bell-shaped curve was not seen for this system. It is possible the melittin unfolded when encapsulated in this system which interfered with the structure of the BMEs as well. System 2 was not analyzed
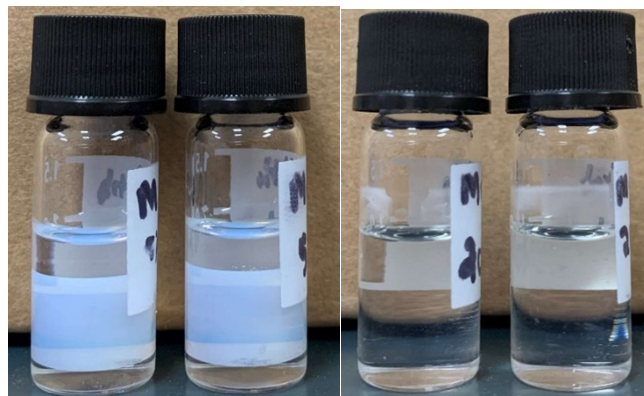
Figure 33. Systems 1C (left) and 1A (right) with the addition of melittin at 1.0g/L
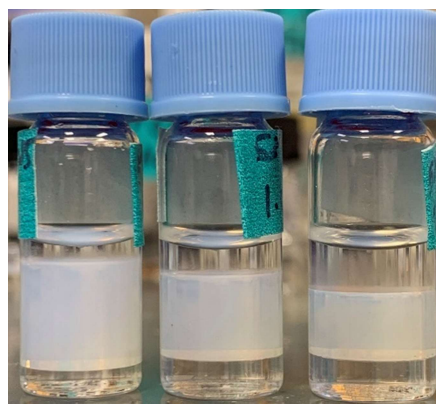
Figure 34. System 1 C with 0, 1.0, and 2.0 g/ L melittin left to right

Table 5. Melittin Concentration in Middle Phase of System 1C and Corresponding Water and Oil Fractions

Melittin Concentration	Percent Melittin Extracted to Middle Phase	Volume % of Middle BME Phase of Overall System	Volume % of Water in BME Phase	Volume % Oil in BME Phase
0.0 g/L	-	64.0%	49.7%	50.3%
1.0 g/L	99%	50.0%	49.5%	50.5%
2.0 g/L	98%	40.0%	49.3%	50.6%
3.0 g/L	98%	33.3%	65.0%	35.0%
4.0 g/L	99%	28.5%	65.0%	35.0%

*Each system was measured in triplicate and volume percentage for the right 2 columns are not taking surfactants into consideration here for these calculations
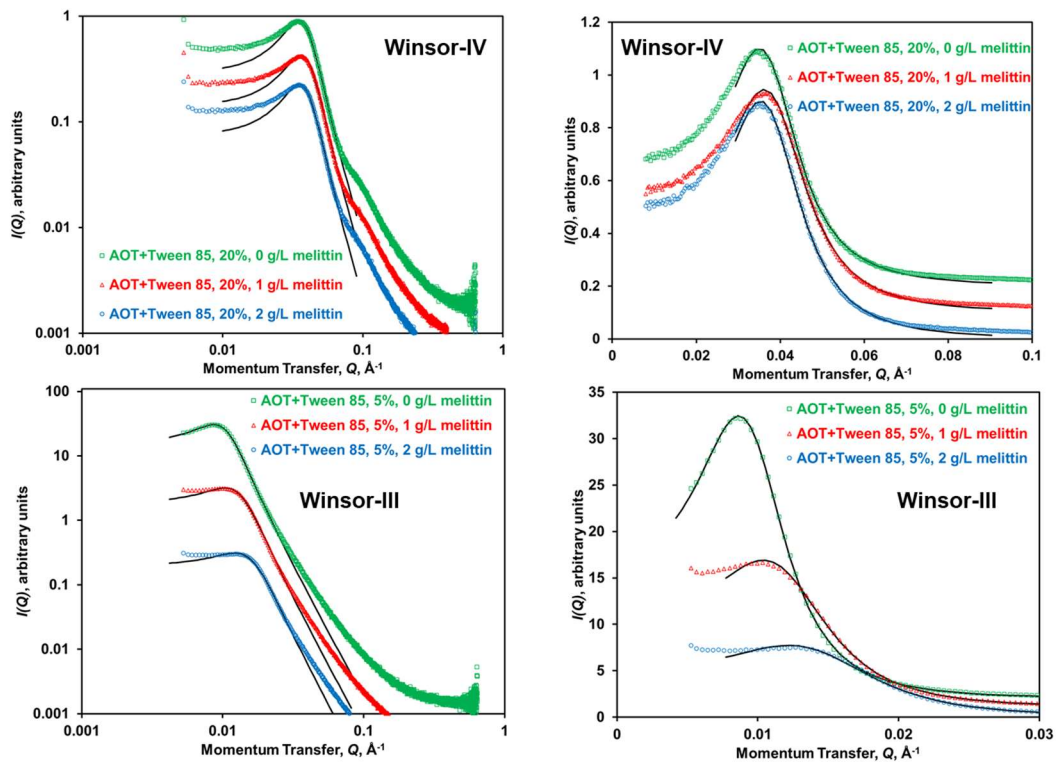
Figure 35. SAXS fitting for system 1C (*left*) and 1A (*right*). Each system had a BME with 0, 1.0, or 2.0 g/L of melittin: data is plotted in log-log (*left*) and rectangular coordinate (*right*)

Table 6. SAXS values calculated from the T-S model for system 1C and 1A

	AOT/Tween 85, W-IV	AOT/Tween 85, W-IV	AOT/Tween 85, W-IV	AOT/Tween 85, W-III	AOT/Tween 85, W-III	AOT/Tween 85, W-III
	0 g/L Mel	1 g/L Mel	2 g/L Mel	0 g/L Mel	1 g/L Mel	2 g/L Mel
correlation length, ξ (Å)	87.8±0.2	82.8±0.2	85.9±0.2	250.6±0.2	182.5±0.2	140.2±0.2
repeat distance, d, (Å)	170.6±0.1	164.8±0.1	169.0±0.1	659.6±0.2	535.1±0.2	444.1±0.2
Amphiphilicity factor, f_a	-0.825	-0.818	-0.821	-0.701	-0.642	-0.595

further because of these results.

SAXS fittings were also completed for system 4 (Fig. 36). x-ray measurements for this system were taken for 0, 0.5, 1.0, 1.5, and 2.0 g/L of melittin in the BME. The values calculated for system 4 varied from system's 1A and 1C. As melittin increased from 0 to 1.0 g/L, the correlation lengths and quasi-periodic repeat distances decreased (Table 7). This showed a decrease in surfactant efficiency with an increase in melittin concentration. However, when the concentration of melittin increased from 1.5 to 2.0 g/L there was an increase in correlation length and quasi-periodic repeat distances (Table 7). Further, the curves for 1.5 and 2.0 g/L are similar to the curves for 0 and 0.5 g/L. This may show that there is an optimal concentration of melittin that system 4 will accept.

3.4.5 CD Spectroscopy

CD measurements for system 1C as a function of melittin concentration and melittin in corresponding aqueous solutions were compared in Figure 37. The graphed lines for the melittin encapsulated within system 1C show a similar shape to the spectra of an alpha helical peptide (Chapter 2, Figure 21). Each of the BME lines have 2 minima around 208 and 225 nm which is typical for the spectra of an alpha helical peptide. The graphed line for melittin in an aqueous solution, partially follows an alpha helical peptide spectrum from 190-215 nm. However, after 215 nm the line shifts to what is expected for a beta-sheet spectra (Chapter 2, Figure 21).

3.4.6 Fluorescence Spectroscopy

Fluorescence emission spectra were used to determine where melittin resided within the BME systems. Figures 38-40 display the spectra for melittin in systems 1C, 1A, and 4, respectively, compared to a melittin in aqueous solution. The fluorescence spectra of melittin underwent a blue shift when encapsulated in BMEs compared to the original aqueous solution. The largest shift was seen in system 1C with a 12 and 14 nm shift to the left for 1.0 and 2.0 g/L melittin. The two W-IV systems had smaller shifts. System 2 fluorescent measurement did not produce the same results (Figure 41). It was hypothesized that melittin was possibly unfolding within system 2 which causing skewed results.
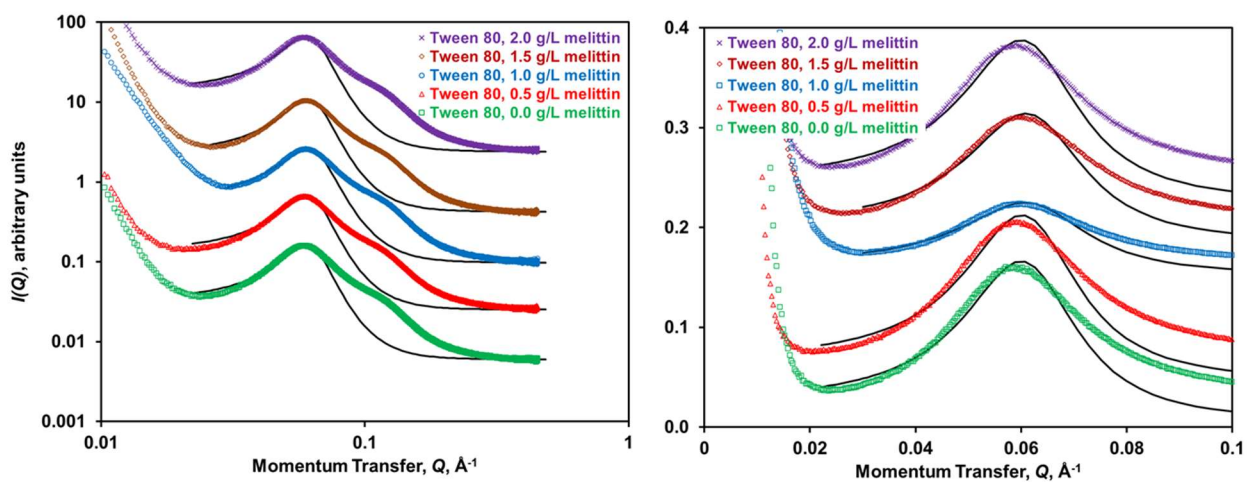
Figure 36. SAXS analysis of BMEs (system 4) containing 0, 0.5, 1.0, 1.5, and 2.0 g/L melittin. Data is plotted in log-log (*left*) and rectangular coordinate (*right*)

Table. 7 SAXS Values Calculated from the T-S Model for System 4

	Tween 80, W-IV	Tween 80, W-IV	Tween 80, W-IV	Tween 80, W-IV	Tween 80, W-IV
	0 g/L Mel	0.5 g/L Mel	1 g/L Mel	1.5 g/L Mel	2 g/L Mel
correlation length, ξ (Å)	75.8±0.2	75.2±0.2	68.4±0.2	72.7±0.2	73.2±0.2
repeat distance, d, (Å)	102.4±	102.1±0.04	100.6±0.04	100.7±0.04	102.2±0.04
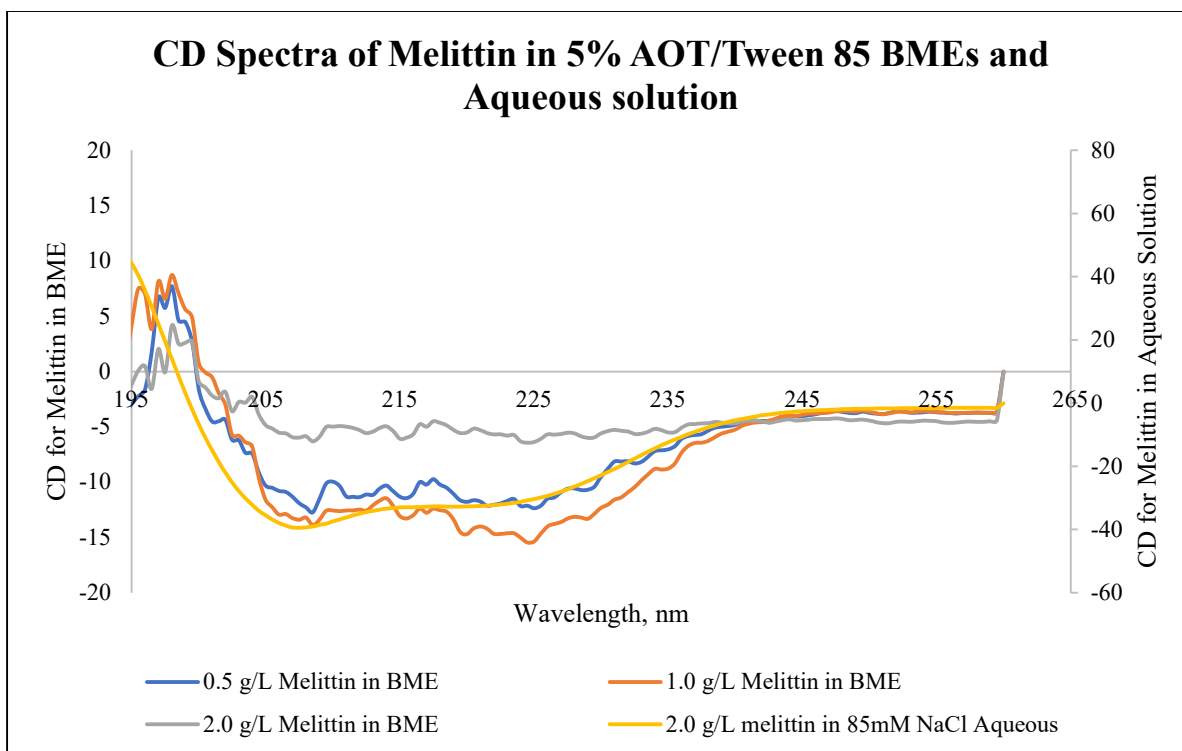
Figure 37. CD spectra of melittin at concentrations of 0.5 (blue line), 1.0 (orange line), and 2.0 (grey line) g/L in system 1C and melittin at 2.0 (yellow line) g/L in an 85 mM aqueous solution
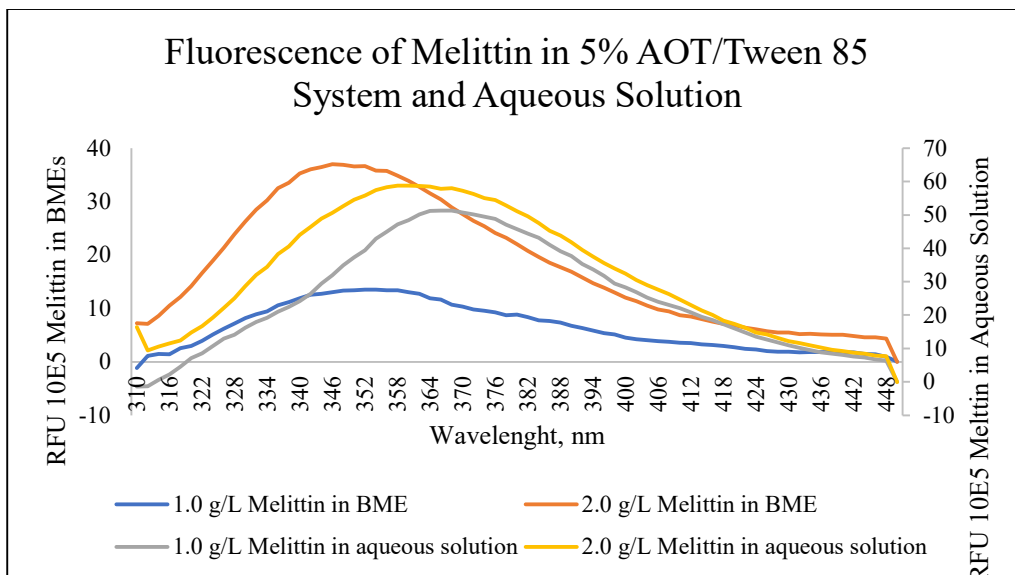
Figure 38. Fluorescence spectra for system 1C with 1.0 and 2.0 g/L melittin and 1.0 and 2.0 g/L of melittin in 85 mM aqueous solution
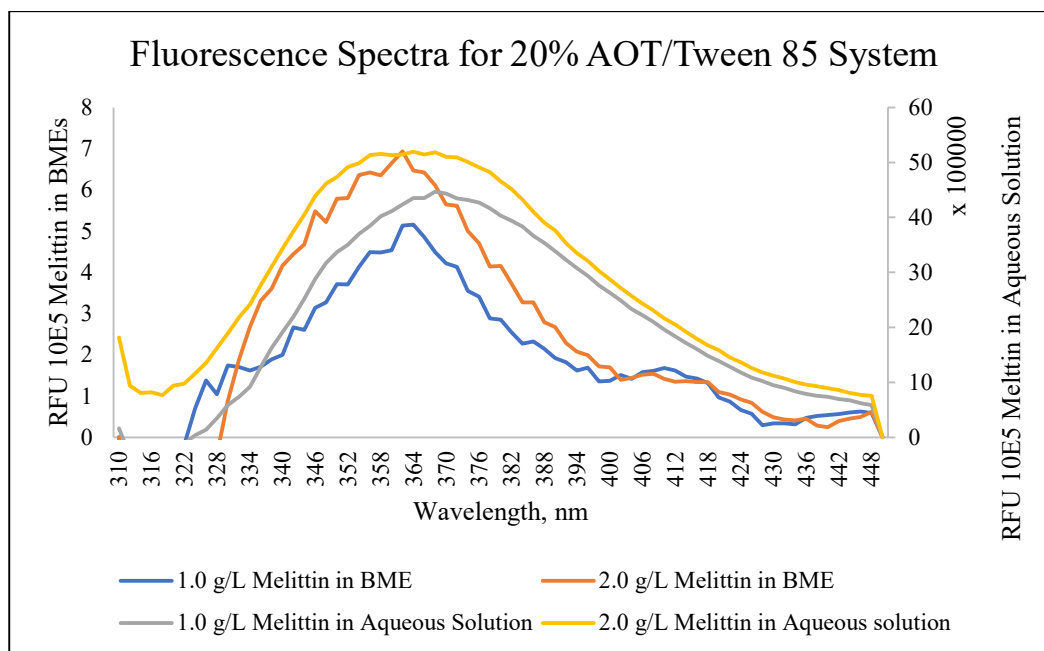
Figure 39. Fluorescence spectra for system 1A with 1.0 and 2.0 g/L melittin and 1.0 and 2.0 g/L of melittin in aqueous solution
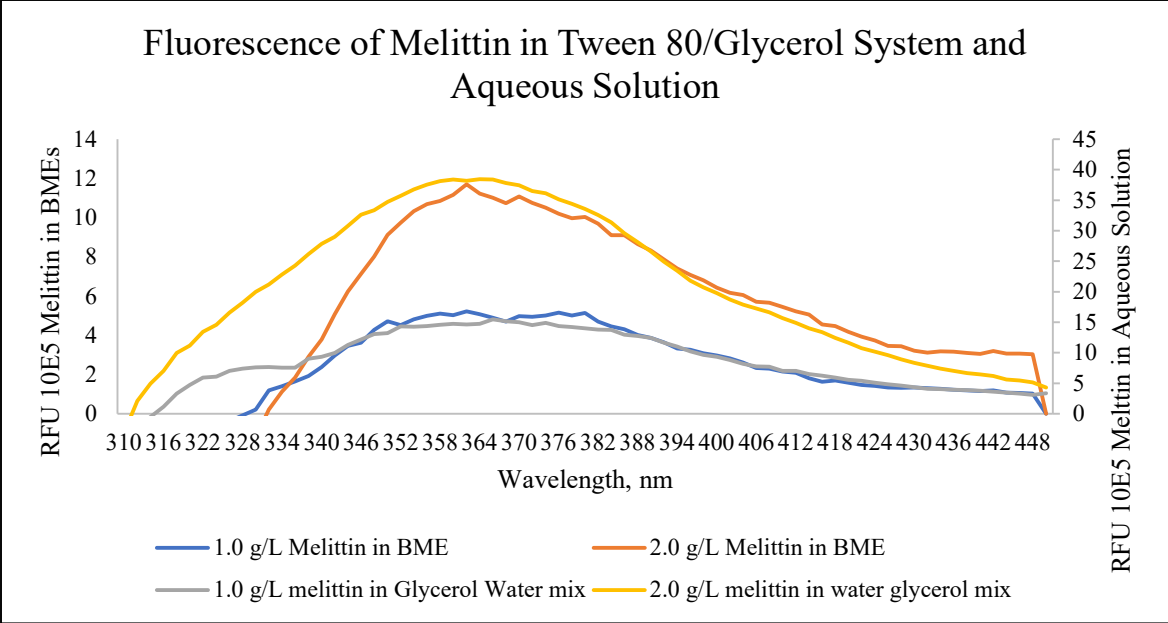
Figure 40. Fluorescence spectra of system 4 with 1.0 and 2.0 g/L melittin and 1.0 and 2.0 g/L melittin in a water/glycerol mixture
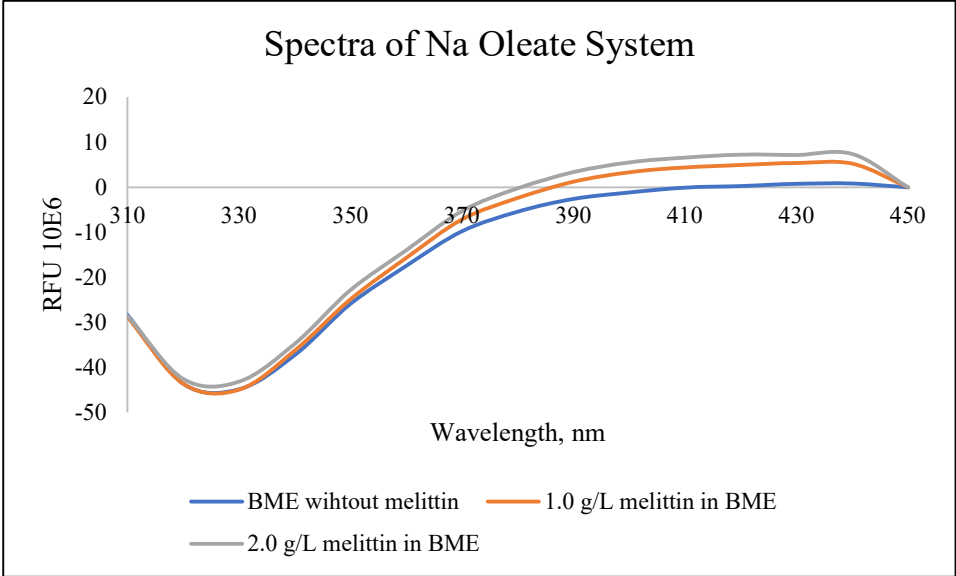
Figure 41. Fluorescence spectra of system 2 with 0, 1.0, and 2.0 g/L melittin

3.4.7 Antimicrobial Assay Results

Dilution and diffusion bioassay techniques were used to assess the bacterial inhibition attributable to melittin loaded BMEs compared to controls. The results gathered from each of the antimicrobial assay trials showed that some assays were more compatible than others with the addition of BMEs. Pitfalls occurred in many of the antimicrobial assays depending on the BME system and the materials and consumables used for the bioassays. Although problems were encountered for bioassays of system 1 and 2, robust results were obtained for system 4.

3.4.7.1 Dilution, Plating, and Optical Density Measurements

In initial testing of the antimicrobial effects of the AMP loaded BMEs, bacterial dilution and plating techniques were used in conjunction with bacterial kinetic measurements. Although the dilution and plating technique are widely used for treatment testing against bacteria, there were mass transfer issues with the AMP loaded BMEs and these methods. Bacterial kinetic readings were successfully taken for bacterial controls, melittin in an aqueous solution, and microemulsion controls (Fig. 42). These graphs show a typical growth curve for bacteria. However, some problems occurred, the first involving the material of the 96 well plate it-self. Initially, a tissue culture treated polystyrene plate was used causing the bacteria cells to adhere to the plate. Then an untreated polystyrene 96 well plate was used for experiments. However, this material caused the BME systems to solidify and adhere to the sides of the wells. From literature review, it is shown that BMEs would react less to polypropylene as the 96 well material (Giacometti et al., 2000). BMEs added the polypropylene well plates aided in reducing the negative effects of the other two plates.

After the plate issue was resolved more issues occurred of unsuccessful treatments. The results gathered showed the bacteria thrived with and without the melittin loaded BME treatments. An experiment was conducted by adding components that are typically added to the well, to a glass vial and visually observing to see what occurred. It was discovered that the broths, which are high in salinity, were causing the BMEs to shift from W-III or W-IV to W-I or W-II. It was hypothesized that this change in microemulsion structure did not allow for the transfer of AMP to the bacteria, resulting in minimal effects of the treatments. It was concluded
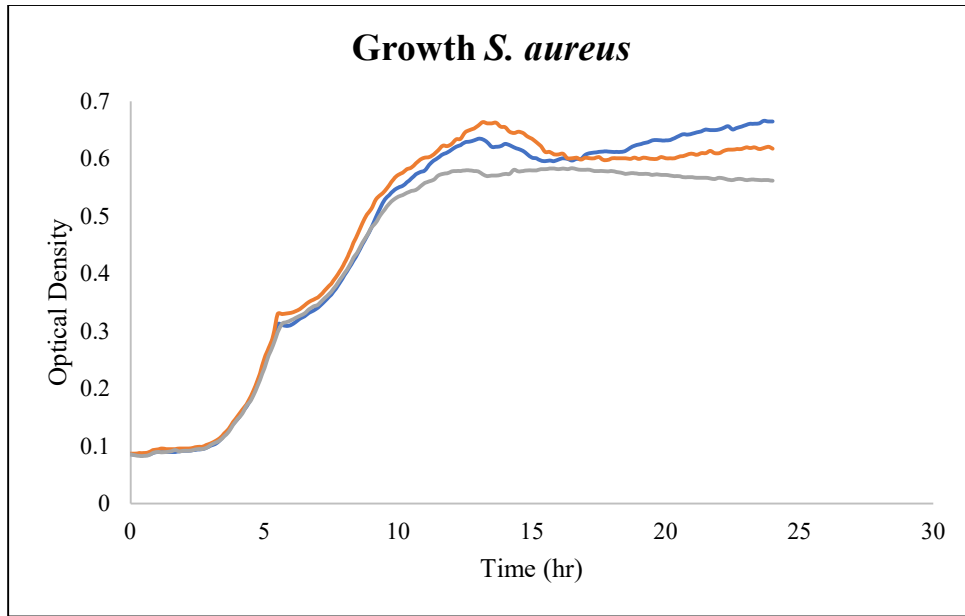
Figure 42. Growth curve of *S. aureus*: optical density plotted over 24 hours of a bacteria culture in a 96 well plate with PBS and TSB, each series represent a replicate of a well with the same components

that other methods, such as diffusion assays, were required to test the AMP loaded BME systems for antimicrobial susceptibility.

3.4.7.2 Disk and Well Diffusion Methods

Initial testing of well and disk diffusion was completed using TSA and Minimal M9 media with Noble agar. TSA was prepared according to manufacturer's instructions and 20 mL of agar was added to a petri dish. After 24 h, treatments did not show any inhibition or diffusion throughout the media. The wells from well diffusion strongly adsorbed BMEs formed by system 1A and 1C, likely due to adsorption of AOT. The next media tested was Noble agar with M9 salts to create a media that was less gelatinous than the TSA. It was hypothesized that the TSA prohibited the AMP loaded BMEs because of the ingredients and the amount of gelatin. The new media was less gelatinous; however, spread plating to create a lawn of bacteria caused the media to tear making it unusable. There was also a challenge in obtaining sufficient bacterial growth on the new media. Moving forward it was decided Mueller Hinton Agar (MHA) would be used for the antimicrobial diffusion assays. MHA has been used in diffusion assays before and has shown advantages when compared to TSA because there are less components in the MHA media (Brenner and Sherris, 1972).

Results from initial disk diffusion testing showed minimal inhibition from the treatments except for system 4. An experiment was completed to determine if melittin in an aqueous solution was effective in inhibiting bacterial growth. This experiment revealed melittin in water was effective against bacteria when well diffusion was used but not when disk diffusion was used (Fig. 43). Figure 43 shows the comparison of melittin stock on a disk and melittin stock in a well. From these results, the decision was made to continue using well diffusion over disk diffusion.

For systems 1A and 1C, there were minimal zones of inhibition around the wells. It was hypothesized that the AOT within these systems was creating a coating around the wells which served as a barrier, thereby prohibiting melittin from diffusing into the media. Figure 44 shows a well diffusion experiment for *P. aeruginosa* using system 1C BMEs. At the bottom of this figure there are three wells that have a white coating around the perimeter of the well. It was

80
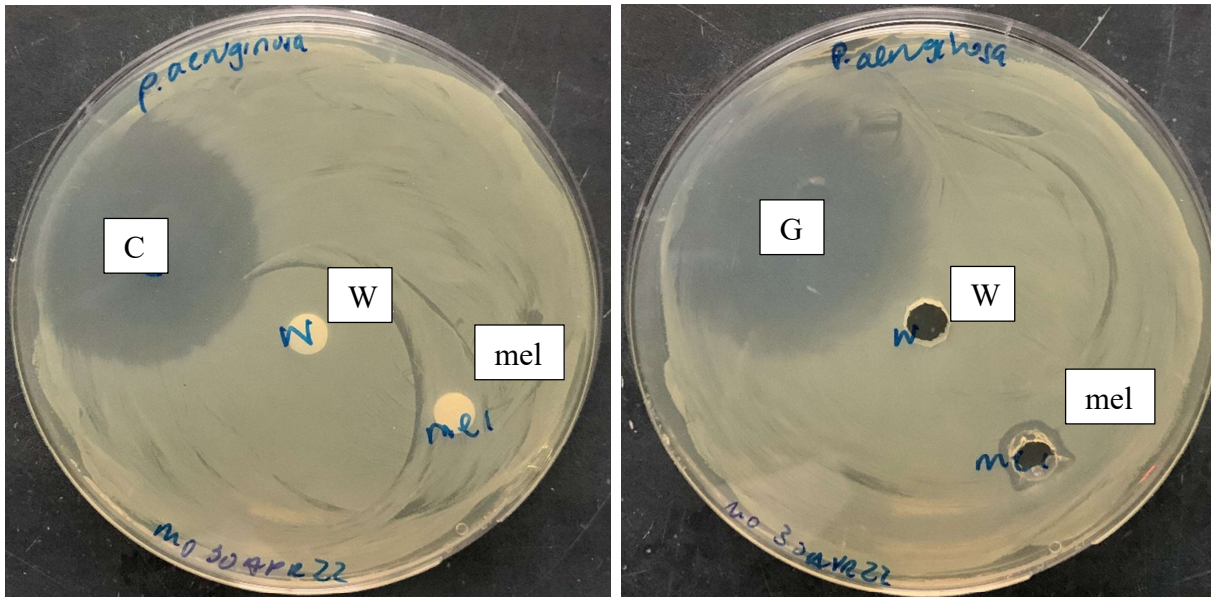
Figure 43. *P. aeruginosa* **treated with disk diffusion (left) and well diffusion (right); on the left treatments are labeled as c (ciprofloxacin), w (water), mel (2 g/L melittin in aqueous solution); on the right treatments are labeled as G (gentamicin), w (water), mel (2 g/L melittin in aqueous solution. The size of the wells are 5 mm in diameter**
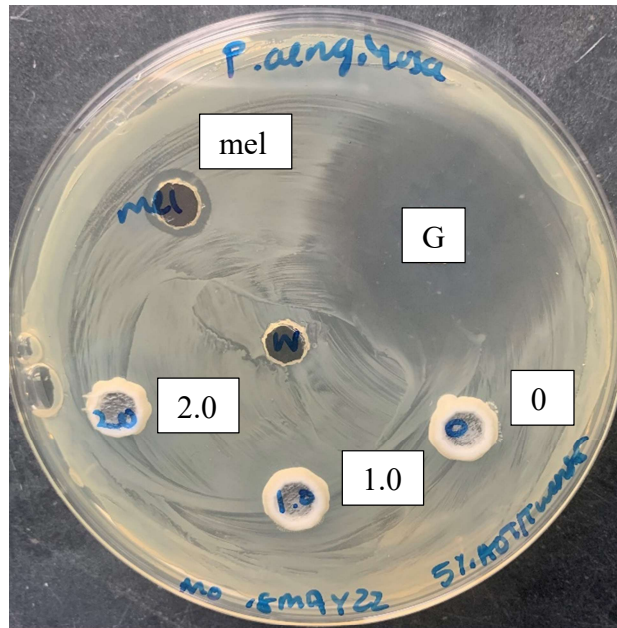
Figure 44. Well diffusion assay against *P. aeruginosa* using system 1C where wells are 5 mm in diameter and the treatments are: mel (2.0 g/L melittin in an aqueous solution), G (gentamicin), 2.0 (2.0 g/L melittin in the BME), 1.0 (1.0 g/L melittin in the BME), and 0 (BME without melittin)

hypothesized the coating was mainly composed AOT. System 4 BMEs successfully diffused through the MHA agar and created zones of inhibition with and without melittin. Figure 45 shows a well diffusion experiment for *A. baumannii* using system 4. There are zones of inhibition around all the treatments. The zone for BMEs formed using for 2.0 g/L melittin is larger than the BME without melittin. This showed that melittin was having an increased inhibitory effect on the bacteria when encapsulated in the BME. Moving forward with antimicrobial assays, only system 4 BMEs were used to gather well diffusion results.

2.4.7.1 System 4 Well Diffusion Results

System 4 BMEs were applied to *S. pyogenes, A. baumannii, E. faecium, P. aeruginosa, S. aureus, and E. coli* K12 in well diffusion. Zones of inhibition were recorded and displayed in Table 8. Error bars were calculated using a 95-confidence interval which are also displayed in Table 8. For each bacterium, there was an increase in zone diameter of the BME with melittin compared to the BME without melittin.

3.4.8 Statistical Analysis Results

Zones of inhibition were found for system 4 created with and without melittin. Therefore, statistical analysis was required to determine if there was a significant difference between the treatments with and without melittin. A one-tailed comparison T test was applied to compare the 1.0 g/L and 2.0 g/L of melittin loaded BME treatments to the BME without melittin. A 95% confidence interval and a p-value of <0.05 was used as significant (Table 9). Table 9 displays the bacteria and whether the corresponding treatment was significantly different to the BME without melittin. All but 5 of the treatments were significantly different (p-value < 0.05). The varied treatments against two bacteria, *A. baumannii* and *E. faecium*, were found to show no significant differences when a 95% confidence interval was used (p > 0.05). When a 90% confidence interval was used, all treatments showed a significant difference except for the 2.0 g/L on *S. pyogenes* (Table 10).
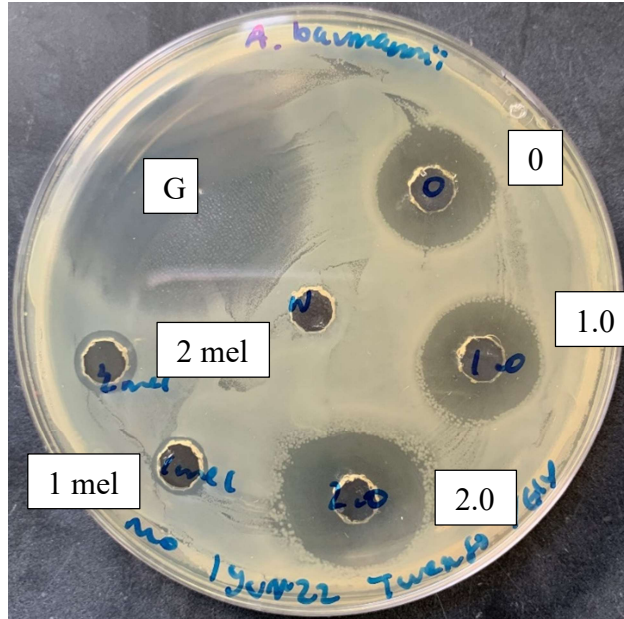
Figure 45. Well diffusion assay against *A. baumannii* using system 4 as a treatment: wells are 5mm in diameter and treatments are as followed G (gentamicin), 0 (no melittin in system 4), 1.0 (1.0 g/L of melittin in system 4), (2.0 g/L of melittin in system 4), 1 mel (1.0 g/L of melittin in an aqueous solution), 2 mel (2 g/L of melittin in an aqueous solution, w (water)

Table 8. Zones of Inhibition for Well Diffusion of each Treatment and System 4 BME (mm) where BME 0, 1, and 2 represent the g/L of melittin within the BME and 1 mel and 2 mel represent the g/L of melittin in an aqueous solution

	Bacteria Strain					
	Gram-negative Bacteria			Gram-positive Bacteria		
Treatment	*E. coli* K12	*A. baumannii*	*P. aeruginosa*	*E. faecium*	*S. aureus*	*S. pyogenes*
Gentamicin[a]	30.67 ±0.45	30.33±0.96	30.50 ± 0.39	30.25 ± 0.89	28.67 ± 0.38	31.17± 0.79
Water[b]	0	0	0	0	0	0
BME 0	12.67 ±0.19	14.00±0.24	13.50 ± 0.20	14.67 ± 0.30	13.83 ± 0.28	14.17 ± 0.28
BME 1	14.00 ± 0.24	14.67±0.30	14.33 ± 0.19	15.50 ± 0.39	14.67 ± 0.30	15.33 ± 0.19
BME 2	13.50 ± 0.20	14.67± 0.38	14.67 ± 0.30	15.17 ± 0.15	14.50 ± 0.20	14.83 ± 0.44
1 mel	2.00 ± 0.00	2.50± 0.20	2.33± 0.38	2.17 ± 0.15	2.00 ± 0.00	1.50 ± 0.20
2 mel	5.00 ± 0.00	4.00 ± 0.28	4.17 ± 0.15	4.17 ± 0.15	4.00 ± 0.00	4.83 ± 0.15

*Zones were corrected by subtracting the diameters of the well, 5 mm, from each measurement

**Standard error was calculated using a 95% confidence interval

a- positive control, b- negative control

Table 9. T-test Results of Significance for System 4 BMEs with Melittin Compared to 0 g/L melittin BME treatment using a 95% confidence interval

Bacteria	1.0 g/L treatment	2.0 g/L treatment
E. coli K 12	Significant	Significant
A. baumannii	Not Significant	Not Significant
P. aeruginosa	Significant	Significant
E. faecium	Not Significant	Not Significant
S. aureus	Significant	Significant
S. pyogenes	Significant	Not Significant

*Differences were considered significant with a p-value < 0.05

Table 10. T-test Results of Significance for System 4 BMEs with Melittin Compared to 0 g/L melittin BME treatment using a 90% confidence interval

Bacteria	1.0 g/L treatment	2.0 g/L treatment
E. coli K 12	Significant	Significant
A. baumannii	Significant	Significant
P. aeruginosa	Significant	Significant
E. faecium	Significant	Significant
S. aureus	Significant	Significant
S. pyogenes	Significant	Not Significant

*Differences were considered significant with p-value <0.1

3.5 Discussion

3.5.1 BME Creation

Five BME systems were successfully identified and created with biocompatible materials. System 1 used a mixed nonionic and anionic surfactant system. System 1A BMEs formed within a minute of adding all the components together. System 1C BMEs also formed quickly, in around 15 minutes. System 1B did not form as quickly, and therefore was not chosen moving forward in the project. System 2 used the anionic surfactant, sodium oleate, and was also a W-IV system. System 3 used a zwitterionic surfactant, lecithin, and created a W-III system. However, this system was slow to equilibrate, and it was decided it would not be used with the addition of melittin. System 4 used a nonionic surfactant, Tween 80, as the main surfactant. This system also formed a W-IV system within a minute. System 5 used lecithin as the surfactant and 1-propanol as a cosurfactant to create a W-IV system. Although it formed within a few minutes, this system had a low overall weight percentage of water. It was decided that this system would not be included for the addition of melittin. These results completed the objective of identifying multiple BMEs created with biocompatible materials.

3.5.2 Cytochrome C Addition to BMEs

Cytochrome c was added to each of the BMEs identified. Cytochrome c is a membrane associated protein that is cationic at a pH<[pI]. Although it is not the same as an AMP, it has similar features that were used as a control to determine if the identified BMEs would accept a protein into the system. Additionally, AMPs are expensive especially compared to cytochrome c. The addition of cytochrome c was a pertinent step towards adding an AMP to reduce the costs and/or need of purchasing large quantities of an AMP. Cytochrome C was successfully accepted into each of the systems as displayed in the results section. It did not cause any significant visual changes to the BME. This was ideal because it meant the addition of an AMP would likely be successful.

3.5.3 Melittin Addition to BMEs

Melittin, a model AMP originating from bee venom was the chosen AMP to add to the identified BMEs. System 1A, 1C, 2, and 4, were chosen for the addition of melittin. Aqueous solutions of 0.5, 1.0, and 2.0 g/L of melittin were added to the BMEs. Visually, melittin was accepted into the W-IV systems without any significant phase changes. For system 1C, the salinity was initially 100 mM NaCl. With the addition of melittin, the system turned into a W-I because the melittin made the surfactants more hydrophilic. A series of trials with salinity's concentrations ranging from 60 mM to 100 mM NaCl was carried out. At 85 mM NaCl, a W-III system was achieved with all three concentrations of melittin tested. Additionally, for system 1C, lower concentrations of the surfactant were tested. But it was determined that 5% surfactant concentration was the optimal concentration to create a W-III. These results completed the objective of successfully encapsulating an AMP into the BMEs.

For system 1C, the concentration of melittin extracted to the middle phase was measured. It was determined that greater than 98% of melittin was encapsulated in the middle bicontinuous phase. These results supported the hypothesis of an AMP being extracted to the bicontinuous phase of the W-III system due to electrostatic forces. Further, these results were ideal because this proved majority of the melittin was being extracted into the middle phase, which would make it the most effective treatment.

3.5.4 SAXS, CD Spectroscopy, and Fluorescence Spectroscopy

Molecular characterization was used to determine important characteristics of the BMEs and melittin within the BMEs. SAXS results displayed melittin had an effect on each of the BMEs. The most significant effect was seen in system 1C. System 1C had the largest decrease in quasi-periodic repeat distance and correlation length with an increase in melittin. This occurred because system 1C had the lowest percentage of surfactant concentration. As melittin increased in system 1C, the surfactants ability to solubilize oil and water was reduced. This was also shown in Figure 34, the middle bicontinuous phase became smaller when a higher concentration of melittin was added. System 1A showed a similar trend; as the concentration of melittin increased, the quasi-periodic repeat distance and correlation length decreased. Although it

showed a similar trend, it was a far less significant difference compared to system 1C. This occurred because system 1A is a W-IV and has a larger concentration of surfactant for melittin to interact with. System 2 displayed irregular SAXS results. This possibly occurred because of the interaction with melittin and the surfactant. It was hypothesized that melittin unfolded within system 2 which caused the unexpected SAXS outputs.

System 4 had some interesting SAXS outputs. There was a decrease in quasi-periodic repeat distance and correlation length from 0-1.0 g/L of melittin, followed by an increase in those lengths from 1.5-2.0 g/L melittin. Melittin seems to have the largest impact on the BME structure (system 4) from 0-1.0 g/L. This suggests a possible maximum acceptance of melittin concentration at 1.0g/L in system 4. It can be hypothesized that melittin has a threshold of acceptance into the W-IV surfactant monolayers. In the antimicrobial assays, it was found that 1 g/L was as successful or sometime more successful in prohibiting bacteria growth than the 2 g/L treatments. These results correlate with the SAXS outputs and if successful, it would save on costs because less AMP would be required.

CD data was collected for system 1C only. Since the other systems were W-IV and higher in surfactant concentration, the CD outputs were noisy and unusable. Displayed in Figure 33 were the CD outputs for melittin within the BME compared to melittin in an aqueous solution. All three BMEs with melittin had two minima occurring at 208 and 225 nm. This is the typical spectra for an alpha-helical peptide. Melittin in an aqueous solution also had a minimum at 208 nm, but the line after 215 nm did not, which aligned more with the spectra for a beta-sheet peptide. This meant that a higher percentage of melittin was in its most active state when encapsulated in the BME compared to the aqueous solution. This supported the hypothesis that BMEs would act as a biomimetic membrane system because melittin was in its most active structure, alpha helix.

Fluorescence measurements were collected for systems 1A, 1C, 2, and 4. The outputs for system 2 were not typical for a fluorescent spectrum. These results further confirmed a possible unfolding of melittin within this system. System 2 was not tested for antimicrobial effectiveness because of these results. For system 1A, 1C, and 4 a blue shift in their respective fluorescence spectrums were seen. A blue shift in fluorescence signifies the location of melittin transition to a more apolar environment when encapsulated in a BME compared to an aqueous solution. This

meant that the melittin was residing between the surfactant monolayers of the BME systems. These results meant, melittin was interacting with the surfactant. This confirms the forces accepting melittin into the BMEs were due to the surfactants.

3.5.5 Antimicrobial Assays

Microtiter dilution, plating, disk diffusion, and well diffusion assays were all tested to determine the antimicrobial effects of the melittin loaded BMEs. Performing antimicrobial assays to test BMEs is not widely researched. There were a few challenges encountered during testing, however, some beneficial results for one of the melittin loaded BMEs were still obtained. In the dilution testing, the addition of TSB and PBS to the loaded microemulsions caused a change in the BME structure. Both of those solutions are high in salinity which has great effects on microemulsions. There were also issues of 96 well plate materials. Some of the BMEs were attracted to the materials causing a residue to occur around the wells. This also made it challenging to determine if the systems weren't effective or if something else was occurring. Although there was no observable inhibition from the melittin loaded BME systems for dilution testing, other assays were required to make final conclusions.

Disk and well diffusion were two other methods attempted to show microbial inhibition for the melittin loaded BMEs. Issues also occurred for disk and well diffusion, especially for systems 1A and 1C. The first issue occurred with the chosen media. TSA had too many components and therefore skewed the results gathered for disk and well diffusion. The customized media did not have enough agar stiffness to withstand the force of spread plating. MHA served as the best media option for disk and well diffusion. Although it has similar gelatinous properties as TSA, the ingredients in MHA are far less, which allowed for better diffusion. For disk diffusion there was not a significant amount of diffusion for system 1A and 1C from the paper disk. In addition, for well diffusion, the AOT caused a build-up of the microemulsion on the sides of the wells. Our hypothesis is that this build-up on the wells blocked the melittin from diffusing through the media, which resulted in the minimal to no inhibition that was observed. System 4 was successful in diffusing into the lawns of bacteria. System 4 showed inhibition with and without melittin. With melittin, the zones of inhibition were increased. For most of the samples, there was a significant difference between the BME with and without

90

melittin. This supports the idea that melittin increased the effectiveness of the BMEs ability to inhibit bacterial growth.

When a 95% confidence interval was used, *A. baumanii* and *E. faecium* showed no significant differences in their zones of inhibition when treated with the BME with and without melittin. However, they were significant if a 90% confidence interval was used (p= 0.06 and 0.08). Ideally, researchers favor using a 95% confidence interval. Though occasionally a 90% confidence interval can be used for smaller experimental sets. The statistical analysis was conducted on 3 replications of the treatment on the bacteria. More replications could be done to further conclude the significance of the difference in zones of inhibitions among the treatments.

3.6 Conclusions

BMEs can be created with biocompatible materials. BMEs were also successful in encapsulating melittin, a model AMP. System 1C extracted >98% of the melittin to the middle phase. These results support the idea that when other AMPs are added, they will likely be accepted. SAXS data concluded melittin had an effect on the BME structures by reducing the surfactants efficiency in system 1C. For system 1A and 4 the efficiency decreased from 0-1 g/L melittin then increased from 1-2 g/L melittin. This meant, there is a limit to the concentration of melittin added to these systems. CD data showed a larger percentage of melittin was more active in the BME compared to an aqueous solution. It was concluded that this would make it an effective topical treatment. Fluorescence data showed melittin resided within the surfactant monolayers of the BMEs. Antimicrobial data showed promising results for system 4 using well diffusion. Statistical analysis showed well diffusion results were statistically different for the melittin loaded BME compared to the BME without melittin. Future research may focus on additional testing to increase statistical significance. Conclusions on antimicrobial effects of system 1A and 1C could not be made. Additional research is required to determine another way to test the inhibition of AMP loaded BMEs. It was difficult because many factors affect microemulsion structure. Additionally, there is limited research data available in literature on BMEs and antimicrobial assays.

This research showed promise in using BMEs as a drug delivery system to host AMPs. From this project it was determined that AMPs are more active when encapsulated in BMEs and

are successful in prohibiting bacterial growth. It was pertinent to determine systems that are biocompatible so that they would not irritate the skin when applied topical. This research was successful in encapsulating melittin in multiple biocompatible BMEs which will hopefully lead to additional research towards using BMEs to encapsulate and deliver other AMPs. Although there was some difficulty in testing BMEs with antimicrobial assays, beneficial progress was made towards finding a way to test for bacterial inhibition. With additional research, better procedures may arise to determine if AMP loaded BMEs can be implemented as a treatment to combat SSIs and chronic wounds.

CHAPTER 4: CONCLUSIONS AND FUTURE WORK

4.1 Conclusions and Future Work

As it has been discussed throughout this paper, SSIs and chronic wounds require new treatments to combat the rise in antibiotic-resistant microorganisms. It was stressed that antibiotics are becoming less and less effective. An innovative treatment would allow people to heal faster and reduce the costs of hospital bills. Further, new treatments are required to reduce the extreme discomfort patients obtain due to SSIs and chronic wounds. New potential topical delivery systems containing AMPs have been proposed from the research conducted.

AMPs have been researched for many years mostly focusing on their structure and modality. They are unique because of their mode of action by interacting with the membranes of unwanted hosts causing them to leak and lyse. More recently AMPs have been studied for their use in treatments, yet few have had success due to their difficulty in encapsulating and maintaining an AMP loaded product. The BMEs presented in this project may provide future researchers with knowledge on the addition of an AMP added to biocompatible BMEs. It was shown that melittin was successfully encapsulated within the BMEs and it is hypothesized that other AMPs would follow in suit.

There was success showing inhibition of bacteria using system 4 loaded with melittin. System 4 included Tween 80, limonene, glycerol, water, and ethanol. System 4 worked well in the diffusion assays by diffusing through the media the microorganisms grew on. An increase in inhibition of the bacteria commonly found in SSIs and chronic wounds was seen with the addition of melittin. However, when diffusion tests were completed with systems 1A and 1C, it was difficult to discern the degree of inhibition results. This system contained water, IPM, AOT, and Tween 85. It is believed the surfactant AOT, strongly adsorbed to the agar media which prohibited the melittin from diffusing and interacting with the bacteria tested. System 4, created with a nonionic surfactant, was successful in encapsulating melittin similar to system 1, which was created with an anionic surfactant. Additionally, system 4 was able to induce alpha helicity for melittin without electrostatic interactions. This is another area of these systems that may require additional research. Future experiments may focus on determining more nonionic surfactant based BMEs to encapsulate melittin and other AMPs.

There were also challenges in molecular characterization for CD spectroscopy when attempting to measure W-IV systems. Further research is necessary to determine the structures of

the AMPs without W-IV BMEs. An additional area of research for these systems would be to characterize the BMEs using SANS. Since a large percentage of BMEs is water, SANS measurements would allow for more accurate readings because neutrons provide a greater scattering length density between the hydrophilic and lipophilic subphases. Further, SANS would allow for selective deuteration of water or oil to control the neutron contrast.

Additional research will need to be completed to determine the cytotoxic effects of AMP loaded BMEs. Research will also need to be conducted on the BMEs interaction with skin. Skin holds complex properties that would likely alter the structure of BMEs. It is possible these systems could also be used on surfaces to prepare hospital instruments instead of skin. Currently the BMEs consist of fluid properties. One way to stabilize the BMEs may be to add a component to create a gel. This research could also be continued to add other components to the BMEs in conjunction with melittin, such as antiseptics. BMEs solubilize both water and oil which would allow any drug that is hydrophilic or lipophilic to be accepted into the system. Future studies may also focus on the release kinetics of the AMP from the BMEs.

At this point, the largest challenge would be determining a suitable antimicrobial assay to determine the effectiveness of the AMP loaded BMEs or a way to manipulate the available assays to work with BMEs. Another option would be to determine other BME systems similar to system 4 that would work well with the antimicrobial assays. Combining BMEs and antimicrobial assays is a fairly new area of research and with more experiments, there may be additional beneficial results. This project has provided a good basis for the many possibilities of AMP loaded BMEs.

REFERENCES

Abbott, S. (2015). *Surfactant science: principles and practice*.

Agency for Healthcare Research and Quality (AHRQ). (2019). Surgical site infections. Patient Safety Network. https://psnet.ahrq.gov/primer/surgical-site-infections

Anil, L., Kannan, K. (2018). Microemulsion as drug delivery system for peptides and proteins. *Journal of Pharmaceutical Sciences and Research.*

Bahar, A. A., Ren, D. (2013). Antimicrobial peptides. *Pharmaceuticals.,* 6, 1543-1576. https://doi.org/10.3390/ph6121543

Bagnall, N. M, Vig, S., Trivedi, P., (2009). Surgical-site infection. *Surgery*. 10.1016/j.mpsur.2009.09.007

Berk, Z. (2018). Chapter 11 – Extraction. *Food Science and Technology*. 10.1016/B978-0-12-812018-7.00011-7

Brenner, V. C., Sherris, J. C., (1972). Influence of different media and bloods on the results of diffusion antibiotic susceptibility tests. *Antimicrobial Agents and Chemotherapy*. 10.1128/aac.1.2.116

Bucki, R., Leszczynska, K., Namiot, A., Sokolowski, W. (2009). Cathelicidin LL-37: a multitask antimicrobial peptide. *Arch. Immunol. Ther. Exp.*, 58:15-25. 10.1007/s00005-009-0057-2

Centers for Disease Control and Prevention (CDC). (2019). *Acinetobacter.* U.S. Department of Health & Human Services. https://www.cdc.gov/hai/organisms/acinetobacter.html

Centers for Disease Control and Prevention (CDC). (2014). *E. coli (Escherichia coli)*. U.S. Department of Health & Human Services. https://www.cdc.gov/ecoli/index.html

Centers for Disease Control and Prevention (CDC). (2019). Methicillin-resistant *Staphylococcus aureus* (MRSA). U.S. Department of Health & Human Services. https://www.cdc.gov/mrsa/index.html

Centers for Disease Control and Prevention (CDC). (2019). *Pseudomonas aeruginosa.* U.S. Department of Health & Human Services. https://www.cdc.gov/hai/organisms/pseudomonas.html

Centers for Disease Control and Prevention (CDC). (2021). *Streptococcus pyogenes* (group A streptococci). U.S. Department of Healthy & Human Services. https://www.cdc.gov/streplab/groupa-strep/index.html

Corswant, C. V., Thoren P. E. G. (1999). Solubilization of sparingly soluble active compounds in lecithin-based microemulsions: influence on phase behavior and microstructure. *Langmuir*. 10.1021/la980706v

de Campo, L., Yaghmur, A., Garti, N., Leser, M. E., Folmer, B., Glatter, O., (2001). Five-component food-grade microemulsions: structural characterization by SANS. *Colloid and Interface Science*. 10.1016/j.jcis.2004.02.027

Senesi, N. and D'Orazio, V., (2005). Fluorescence spectroscopy. *Encyclopedia of Soils in the Environment*. 10.1016/B0-12-34853-4/00211-3

Dijksteel, G. S., Ulrich, M. M. W., Middlekoop, E., Boekema, B. K. H. L., (2021). Review: lessons learned from clinical trials using antimicrobial peptides (AMPs). *frontiers in Microbiology.* 12:616979. 10.3380/fmicb.2021.616979

Fife, C. E., Cater, M. J. (2012). Wound care outcomes and associated cost among patients treated in US outpatient wound centers: data from the US wound registry. *Wounds*.

Frykberg, R. G. and Banks, J., (2010) Challenges in the Treatment of Chronic Wounds. *Advances in Wound Care.* 10.1089/wound.2015.0635

Giacometti, A., Cirioni, O., Barchiesi, F., Del Prete, M. S., Fortuna, M., Caelli, F., Scalise, G., (2000). In vitro susceptibility tests for cationic peptides: comparison of broth microdilution methods for bacteria that grow aerobically. *Antimicrobial Agents and Chemotherapy*. 10.1128/aac.44.6.1694-1696.2000

Goebel, A., Neubert, R. H. H., (2008). Dermal peptide delivery using colloidal carrier systems. *Skin pharmacology and physiology.* 10.1159/000109082

Gogoladze, G., Grigolava, M., Vishnepolsky, B., Chubinidze, M., Duroux, P., Lefranc M. P., Pirtshkalava, M., (2014). DBAASP: database of antimicrobial activity and structure of peptides. *FEMS Microbiology Letters,* 10.1111/1574-6968.12489

Gottler, L. M., Ramamoorthy, A. (2008). Structure, membrane orientation, mechanism, and function of pexiganan – a highly potent antimicrobial peptide designed from magainin. *Biochimica et Biophysica Acta.,* 1788, 1680-1686. https://doi.org/10.1016/j.bbamen.2008.10.009

Gupta, B. B., Soman, K., Bhoir, L., Gadahire, M., Patel, B., Ahdal, J. (2021). The burden of methicillin resistance *Staphylococcus aureus* in surgical site infections: A review. *Joundal of Clinical & Diagnostic Research*. 10.7860/JCDR/2021/46922.14891

Hayes, D. G., Ye, R., Dunlap, R. N., Anunciado, D. B., Pingali, S. V., O'Neill, H. M., Urban, V. S. (2018). Bicontinuous microemulsions as a biomembrane mimetic system for melittin. *Biomembranes*. 624-632. http://doi.org/10.1016/j.bbamem.2017.11.005

Hayes, D. G., Gomez de Rio, J. A., Ye, R., Urban, V. S., Pingali, S. V., O'Neil, H. M., (2015). Effect of protein incorporation on the nanostructure of the bicontinuous microemulsion phase of Winsor-III systems: a small-angle neutron scattering study. *Langmir*. 10.1155/2017/3647801

Hayes, D. G., (2012). Protein purification using 3-phase microemulsion systems. *A Presentation for the University of Alabama, Huntsville*

Hayes, D. G., Alkhatib, M. H., Gomes del Rio, J., Urband, V. S., (2012). Supplementary Data: physiochemical characterization of water-in-oil microemulsions formed by a binary 1, 3-dioxolan alkyl ethocylate/aerosol-OT surfactant system.

Hirose, A., Terauchi, M., Osaka, y., Akiyoshi, M., Kato, K., Miyasaka, N., (2018). Effect of soy lecithin on fatigure and menopausal symptoms in middle-aged women: a randomized, double-blind placebo-controlled study. *Nutritional Journal*. 10/1186/s12937-018-0314-5

Hammouda, B., (1995). A tutorial on small-angle neutron scattering from polymers.

Jacobson, D., Arif., M., Huffman, P., (2004). A new neutron imaging facility at BT-6 for the non-destructive analysis of working fuel. NIST cells.https://www.ncnr.nist.gov/AnnualReport/FY2003_html/RH2/

Jamasbi, E., Mularski, A., Separovic, F., (2016). Model membrane and cell studies of antimicrobial activity of melittin analogues. *Current Topics in Medicinal Chemistry*., 16, 40-45.

Jantrawut, P., Boonsermsukcharoen, K., Thipnan, K., Chaiwarit, T., Hwang, K., Park, E., (2018). Enhancement of antibacterial activity of orange oil in pectin thin film by microemulsion. *Nanomaterials*. 10.3390/nano8070545

Kegel, W. K., Reiss, H. (1996). Theory of vesicles and droplet type microemulsions: configurational entropy, size distribution, and measurable properties. *Journal of the Chemical Society, Faraday Transactions 2: Molecular and Chemical Physics*. https://doi.org/10.1039/F29817700601

Kline, S. R., (2006). Reduction and analysis of SANS and USANS data using IGOR Pro. *Journal of Applied Crystallography.* 10.1107/S0021889806035059

Klossek, M. L., Touraud, D., Kunz, W. (2012). Microemulsions with renewable feedstock oils. *The Roayl Society of Chemistry.* http://doi.org/10.1039/C2GC35035A

Klossek, M. L., Marcus, J., Tourad, D., Kunz, W. (2013). Highly water dilutable green microemulsions. *Colloids and Surfaces A: Physiochemical and Engineering Aspects*. http://dx.doi.org/10.1016/j.colsurfa.2012.12.061

Leaper, D. J., (2010). Surgical-site Infection. *British Journal of Surgery.* 10.1002/bjs.7275

Liu, H., Wang, Y., Lang, Y., Yao, H., Dong, Y., Li, S., (2009). Bicontinuous cyclosporin A loaded water-AOT/Tween 85-Isopropylmyristate microemulsions: structural characterization and dermal pharmacokinetics in vivo. *Journal of pharmaceutical sciences.* 10.1002/jps.21485

Moghaddam, H. m., Dehghannoudeh, G., Basir, M. Z., (2016). Evaluation of the thermodynamic behavior of nonionic polyoxyethylene surfactants against temperature changes. *Pakistan Journal of Pharmaceutical Sciences*. 29(2), 521-527

Mogi, T., Kita, K., (2009). Gramicidin S and polymyxins: the revival of cationic cyclic peptide antibiotics. *Cellular and Moleclular Life Sciences*. 10.1007/s00018-009-0129-9

Moreno, M., Giralt, E. (2015). Three valuable peptides from bee an wasp venoms for therapeutic and biotechnological use: melittin, apamin, and mastoparan. *Toxins.*, 7, 1126-1150. 10.3390/toxins7041126

Nakama, Y. (2017). Surfactants. *Cosmetic Science and Technology: Theoretical Principles and Applications.* 10.1016/B978-0-12-802005-0.00015-X

Nordström, R., Malmsten, M. (2017). Delivery systems for antimicrobial peptides. *Advances in Colloid and Interface Science,* 242, 17-34. https://dx.doi.org/10.1016/j.cs.2017.01.005

Pachuau, L. (2015). Recent developments in novel drug delivery systems for wound healing. *Expert Opinion on Drug Delivery*. https://doi.org/10.1517/17425247.2015.1070143

Pires, M. J., Aires-Barros, M. R., Cabral, J. M. S. (1996) Liquid-liquid extraction of proteins with reversed micelles. *Biotechnology Progress.* https://doi-org.utk.idm.oclc.org/10.1021/bp950050l

Prenner, E. J., Lewis, R. N. A. H., McElhaney R. N. (1999). Interaction of antimicrobial peptide gramicidin S with lipid bilayer model and biological membranes. *Biochemica et Biophysica Acta.*, 201-221.

Ramirez, L. S., Pande, J., Shekhtman, A., (2018)., Helical structure of recombinant melittin. *The Journal of Physical Chemistry.* 10.1021/acs.jpcb.8b08424

Rijal, N., (2022). Spread plate technique: principle, procedure, results. https://microbeonline.com/spread-plate-technique/

Rosen, M. J. (1989). Surfactants and interfacial phenomena. Location: John Wiley & Sons.

Schäfer-Korting, M., Rolff, J. (2018). Chapter 2, skin delivery of AMP's. In *Emerging Nanotechnologies in Immunology* (pp. 23-45). Berlin, Germany. https://doi.org/10.1016/B978-0-323-40016-9.00002-6

Schubert, K. and Strey, R., (1991). Small-angle neutron scattering from microemulsions near the disorder line in water/formamide-octane-CiEj systems. *Journal of Chemical Physics.* 10.1063/1.461282

Sen, C. K., (2019). Human wounds and its burden: an updated compendium of estimates. *Advances in Wound Care.* 10.1089/wound.2019.0946

Silas, J. A. and Kaler, E.W., (2003). Effect of multiple scattering on SANS spectra from bicontinuous microemulsions. *Journal of Colloid and Interface Science.* 10.1016/S0021-9797()2)00059-0

Silhavy, T. J., Kahne, D., Walker, S., (2010). The bacterial cell envelope. *Cold Spring Harb Perspect Biol.* 10.1101/cshperspect.a000414

Solans, C., Garcia-Celma, M. J. (1997). Surfactants for microemulsions. *Current opinion in colloid & interface science.* 10.1016/S1359-0294(97)80093-3

Spernath, A., Aerin, A. (2007). Microemulsions as carriers for drugs and nutraceuticals. *Advances in Colloid and Interface Science.* 10.1016/j.cis.2006.11.016

Svergun, D. I., Koch, M. H. J., (2003). Small-angle scattering studies of biological macromolecules in solution. *Reports on Progress in Physics.*

Tamhane, V. A., Dhaware, D. G., Khandelwal, N., Giri, A. P., Panchagnula, V., (2012). Enhanced permeation, leaf retention, and plant protease inhibitor activity with bicontinuous microemulsions. *Journal of Colloid and Interface Science.* http://dx.doi.org/10.1016/j.jcis.2012.06.025

Tartaro, G., Mateos, H., Schirone, D., Angelico, R., Palazzo, G. (2020). Microemulsion microstructure(s): a tutorial review. *Nanomaterials*. 10.3390/nano10091657

Tenover, F. C., (2017). Antimicrobial susceptibility testing methods for bacterial pathogens. *Antimicrobial Drug Resistance*. 10.1007/978-3-319-47266-9_32

Teubner, M., Strey, R., (1987). Origin of the scattering peak in microemulsions. *The Journal of Chemical Physics*. 10.1063/1.453006

Thapa, R. K., Diep, D. B., Tønnesen, H. H. (2019). Topical antimicrobial peptide formulations for wound healing: current developments and future prospects. *Acta Biomaterialia.,* 103, 52-67. https://doi.org/10.1016/j.actbio.2019.12.025

Thermo Fisher Scientific Inc. (2017). Protein assay technical handbook. https://assets.thermofisher.com/TFS-Assets/LSG/brochures/protein-assay-technical-handook.pdf

Turnbridge, J. D., (2015). Susceptibility test methods: general considerations. *Manual of Clinical Microbiology 11th Edition.* 10.1128/9781555817381.ch70

Teixeira, V., Feio, M. J., Bastos, M., (2012). Role of lipids in the interaction of antimicrobial peptides with membranes. *Progress in Lipid Research*. 10.1016/j.plipres.2011.12.005

van der Does, A. M., Bergman, P., Agerberth, B., Lindbom, L. (2012). Induction fo the human cathelicidin LL-37 as a novel treatment against bacterial infections. *Journal of Leukocyte Biology.* 10.1189/jlb.0412178

Viyoch, J., Pisutthanan, N., Faikreua, A., Nupangta, K., Wangtorpol, K., Ngokkuen, J., (2006). Evaluation of *in vitro* antimicrobial activity of Thai basil oils and their micro-emulsion formulas against *Propionibacterium acnes*. *International Journal of Cosmetic Scientce*. 10.1111/j.1467-2494.2006.00308.x

Wei, Y., Thyparambil, A. A., Latour, R. A., (2014). Protein helical structure determination using CD spectroscopy for solutions with strong background absorbance from 190 to 230 nm. *Biochim Biophys Acta.* 10.1016/j.bbapap.2014.10.001

Wiegand, I., Hilpert, K., Hancock, R. E.W. (2007). Agar and broth dilution methods to determine the minimal inhibitory concentration (MIC) of antimicrobial peptides. *Nature Protocols*. 10.1038/nprot.2007.521

Winsor, P. A., Hydrotropy, solubilization, and related emulsification processes. *Transactions of the Faraday Society* 1948, 44, 376-82

Woody, R. W., (1995). Circular dichroism. *Methods in Enzymology*. 10.1016/0076-6879(95)46006-3

Yanyu, X., Fang, L., Qineng, P., Hao, C. (2012). The influence of structure and the composition of water/AOT/Tween 85/IPM microemulsion system on transdermal delivery of 5-fluoracil. *Drug Development and Industrial Pharmacy.* http://doi.org/10.3109/03639045.2012.654795

Yuan, J. S., Ansar, M., Samaan, M., Acosta, E. J. (2007). Linker-based lecithin micromeulsions for transdermal delivery of lidocaine. *International journal of pharmaceuticals*., doi:10.1016/j.ijpharm.2007.07.047

Zimlichman, E., Henderson, D., Tamir, O., Franz, C., Song, P., Yamin, C.K. (2012). Health care-associated infections: A meta-analysis of costs and financial impact on the US health care system. *JAMA Internal Medicine*. 10.1001/jamainternmed.2013.9763

VITA

Madison grew up in Elkridge, Maryland. She obtained her Bachelor of Sciences degree in Biosystems Engineering from the University of Tennessee in 2020. She continued her studies at the University of Tennessee to pursue a Master of Science degree in Biosystems Engineering.